RSC Advances

PAPER

View Article Online
View Journal | View Issue

Check for updates

Cite this: *RSC Adv.*, 2020, **10**, 43299

1-Phenyl-*N*-(benzothiazol-2-yl)methanimine derivatives as Middle East respiratory syndrome coronavirus inhibitors†

Min-Qi Hu,‡[a] Heng Li,‡[bc] Ying Lin,[a] Ying Zhang,[a] Jie Tang,[ad] Jian-Ping Zuo,[b] Li-Fang Yu,[a] Xian-Kun Tong,*[bc] Wei Tang*[bc] and Fan Yang*[a]

Received 3rd October 2020
Accepted 20th November 2020

DOI: 10.1039/d0ra08442e

rsc.li/rsc-advances

Middle East respiratory syndrome coronavirus (MERS-CoV) poses a serious threat to human health, and currently there are no effective or specific therapies available to treat it. Herein a series of 1-phenyl-*N*-(benzothiazol-2-yl)methanimine derivatives with inhibitory activity against MERS-CoV are described. The compound **4f** with a 50% inhibition concentration value of 0.09 μM is a promising inhibitor that warrants further evaluation, towards the development of potential anti-MERS-CoV drugs.

Introduction

Middle East respiratory syndrome coronavirus (MERS-CoV) is a novel zoonotic virus in the Middle East.[1,2] It first appeared in Saudi Arabia in June 2012,[3] then spread to the rest of the Middle East and South Korea.[4] MERS-CoV is primarily transmitted from animals to humans,[5] but it can reportedly spread from human to human through close contact.[6,7] It can cause severe respiratory disease, with symptoms of fever, coughing, and dyspnea, and may contribute to severe gastrointestinal diseases and renal failure.[8] As at 03 June 2020, the World Health Organization had reported 2494 laboratory-confirmed cases of MERS-CoV infection, including 858 confirmed deaths (an approximately 35% fatality rate) in over 27 countries.

MERS-CoV poses a severe threat to human health, as illustrated by the recent global coronavirus disease-2019 (COVID-19) pandemic caused by severe acute respiratory syndrome coronavirus 2. Although some reported therapeutics for COVID-19 have recently been reported,[9–17] their curative effect is still very limited and there can be side effects.[18,19] Similarly, despite ongoing global efforts to develop small-molecule inhibitors,[20–26] peptide inhibitors,[27–30] neutralizing antibodies,[31–33] and vaccines[34–36] for the treatment and prevention of MERS-CoV, there is no effective approved specific antiviral therapy for MERS-CoV infection. Therefore, the development of specific antiviral drugs for the treatment of MERS-CoV is urgently needed.

Viral genomic studies indicate that MERS-CoV is an enveloped virus with positive-sense single-stranded RNA that belongs to lineage C in the genus *Betacoronavirus* of the family Coronaviridae under the Nidovirales order.[3] It is the sixth coronavirus known to infect humans, and the first known lineage C *Betacoronavirus* associated with human infection.[37,38] The MERS-CoV genome is approximately 30 kilobases in size and contains more than 10 open reading frames (ORFs).[39] The large replicase ORF1a and ORF1b produce polyproteins PP1a and PP1ab, which are subsequently cleaved into 15 or 16 nonstructural proteins.[40–42] The region downstream of ORF1b encodes at least four main structural proteins: spike (S), membrane (M), envelope (E), and nucleocapsid (N).

The S protein serves as the critical surface-located trimeric glycoprotein of MERS-CoV and induces entry into host cells,[43] and it is composed of subunits S1 and S2. The receptor-binding domain on the S1 subunit attaches to dipeptidyl peptidase 4, which is a well-known target for diabetes.[44–49] The conformation of the S2 subunit then changes and a six-helix bundle fusion core is formed, which enables the formation of the viral envelope, facilitating tight host cell membrane binding for fusion and subsequent host cell entry.[50] Thus the S protein plays a pivotal role in mediating the entry of the virus into target host cells.

According to previous reports, MERS-CoV pseudovirus expressing S protein, which allows for single-cycle infection in cells expressing dipeptidyl peptidase 4, can be used to rapidly screen MERS-CoV entry inhibitors.[51] In the current study, novel small-molecule inhibitors of entry events of pseudovirus expressing S protein were identified *via* high-throughput screening technology using a cell-based assay.

[a]*Shanghai Engineering Research Center of Molecular Therapeutics and New Drug Development, School of Chemistry and Molecular Engineering, East China Normal University, Shanghai, 200062, China. E-mail: fyang@chem.ecnu.edu.cn*

[b]*Shanghai Institute of Materia Medica, Chinese Academy of Sciences, Shanghai, 201203, China. E-mail: tangwei@simm.ac.cn; xktong@simm.ac.cn*

[c]*School of Pharmacy, University of Chinese Academy of Sciences, Beijing, 100049, China*

[d]*Shanghai Greenchem & Biotech Co. Ltd., Shanghai, 200062, China*

† Electronic supplementary information (ESI) available. See DOI: 10.1039/d0ra08442e

‡ These authors contributed equally to this work.

Open Access Article. Published on 07 2020. Downloaded on 2025/12/13 4:57:53.
This article is licensed under a Creative Commons Attribution-NonCommercial 3.0 Unported Licence.

Open Access Article. Published on 07 2020. Downloaded on 2025/12/13 4:57:53.
This article is licensed under a Creative Commons Attribution-NonCommercial 3.0 Unported Licence.

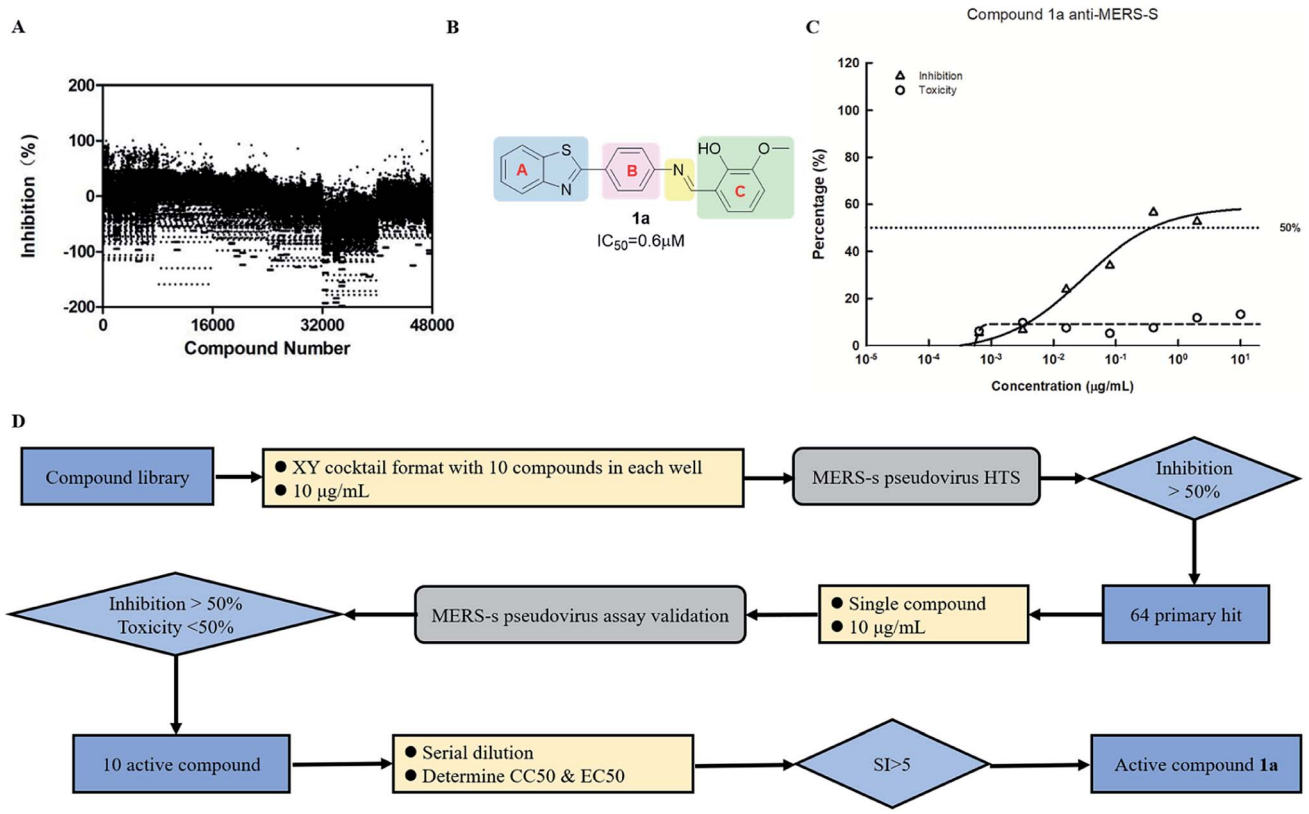

Fig. 1 High-throughput screening output. (A) Data from the 48 000-compound orthogonal cocktail library primary screening experiments were plotted as inhibition of MERS-S pseudovirus infection in Huh-7 cells. Inhibition was calculated as 100% minus the percentage of luciferase readout of each well against the control well with no drug, *i.e.*, 100% − Luc (compound)/Luc (control) × 100%. (B) The structure of the hit compound **1a**. (C) Dose-dependent curve of inhibition activity and toxicity of compound **1a** in a MERS-S pseudovirus assay. (D) Flow chart of the high-throughput screening and validation procedure.

Materials and methods

Screening was performed using an orthogonal cocktail library[52] composed of 48 000 compounds that had never been screened for anti-MERS-CoV activity (Fig. 1A). Compound library samples were orthogonally pooled as mixtures of 10 per well at 2 μg mL^{-1} each, with duplicate representation for each compound (Fig. 1D). This bidirectional orthogonal pooling strategy enables greater screening efficiency and throughput when using large

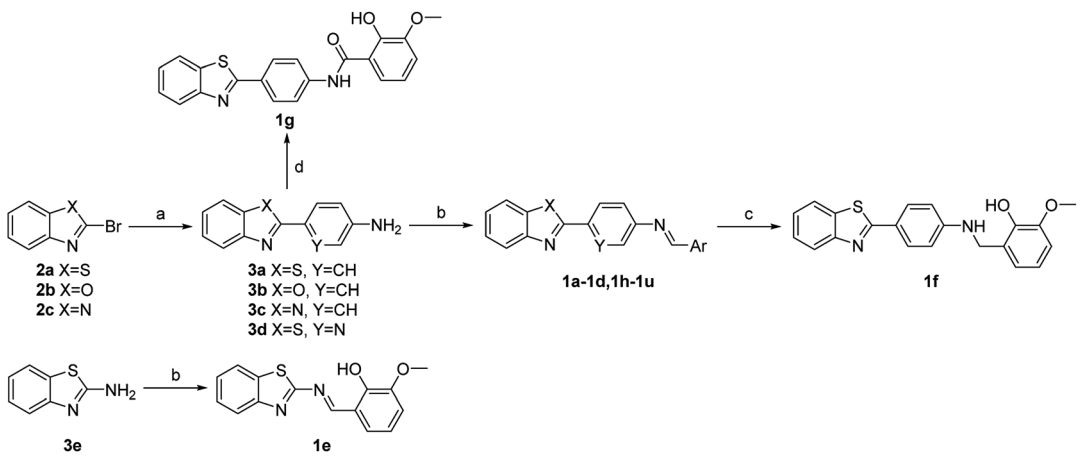

Scheme 1 Reagents and conditions. (a) 4-Aminophenylboronic acid pinacol ester or 5-aminopyridine-3-boronic acid pinacol ester, Pd(dppf)Cl_2·CH_2Cl_2, K_2CO_3, DMF, 70 °C, 16 h. (b) ArCHO, AcOH, MeOH, reflux, 2 h. (c) $NaBH_4$, MeOH, room temperature, 1 h. (d) 2-Hydroxy-3-methoxybenzoyl chloride, $NaHCO_3$, H_2O, Et_2O, room temperature, 12 h.

 This journal is © The Royal Society of Chemistry 2020

Open Access Article. Published on 07 2020. Downloaded on 2025/12/13 4:57:53.
This article is licensed under a Creative Commons Attribution-NonCommercial 3.0 Unported Licence.

compound libraries. Using this approach, compound **1a** was identified as a modest entry inhibitor (Fig. 1B) with a 50% inhibition concentration (IC_{50}) of 0.73 μM (Fig. 1C). Using **1a** as a hit compound, a series of 1-phenyl-*N*-(benzothiazol-2-yl) methanimine derivatives were designed and synthesized, and structure–activity relationships and their inhibitory potencies against MERS-S pseudovirus were investigated.

Results and discussion

Four major regions were partitioned for diversification; the benzothiazole portion (blue), the linker region (pink), the imine portion (yellow), and the phenyl portion (green) (Fig. 1B). Compounds **1a–1g** were synthesized first as outlined in Scheme 1. Commercially available aryl bromides were used as the starting material, and the corresponding intermediate amines **3a–3d** were prepared using the Suzuki–Miyaura cross-coupling reaction.[53] Compounds **1a–1e** were generated using the reaction of an intermediate amine with the corresponding aromatic aldehyde in the presence of AcOH as catalyst.[54] Compound **1g** was generated by the reaction of **3a** with 2-hydroxy-3-methoxybenzoyl chloride. Compound **1f** was generated by a reduction reaction of **1a** with $NaBH_4$.[55] Their IC_{50} values against MERS-S pseudovirus and 50% cytotoxic concentration (CC_{50}) values are summarized in Table 1. The Schiff base structure of hit compound **1a** was confirmed by comprehensive spectral data. The ^{1}H NMR spectrum depicted a sharp singlet peak at δ 8.67 parts per million (ppm) indicating the presence of azomethine proton (–CH═N–). Phenolic-OH proton and methoxy protons exhibited singlet peaks at δ 13.44 and δ 3.94 ppm respectively. A multiplet signal at δ 6.87–8.14 ppm was assigned to the aromatic protons. The ^{13}C nuclear magnetic resonance spectrum of **1a** revealed corresponding peaks in the range of δ 114.2–166.1 ppm which were assigned to azomethine (–CH═N–) carbon and aryl carbons. A peak at δ 55.2 ppm was identical to the methoxy carbon. The ^{1}H–^{1}H COSY spectrum demonstrated chemical shifts of three protons on ring C at δ 6.87–7.06 ppm, and two protons near the nitrogen atom side on ring B at δ 7.36–7.41 ppm. Correlation between the azomethine proton and the two protons near the nitrogen atom side on ring B was observed in the ^{1}H–^{1}H NOSEY correlation spectrum, indicating that the imine moiety of compound **1a** is *E*-geometry. The HRMS (ESI) spectrum of **1a** depicted a signal at *m*/*z* 383.0823, indicating a $[M + Na]^+$ signal with the molecular formula $C_{21}H_{16}N_2NaO_2S$, which is concordant with the structure of **1a**. Characteristic spectra and data are shown in the ESI.†

Compounds with benzoxazole (**1b**) or benzimidazole (**1c**) motifs lost inhibitory activity, as did the compound without

Table 1 Inhibitory activity of **1a–1g** against MERS-S pseudovirus

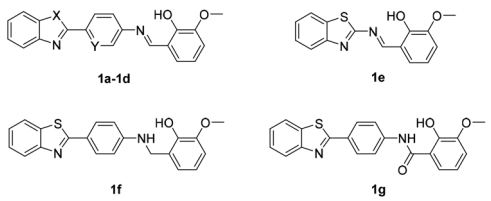

Compound	X	Y	IC_{50}[a]	CC_{50}[b]
1a	S	CH	0.73 ± 0.66	>100
1b	O	CH	>10.0	>100
1c	NH	CH	>10.0	>100
1d	S	N	2.7 ± 0.19	>100
1e	—	—	>10.0	>100
1f	—	—	>10.0	>100
1g	—	—	>10.0	>100
HRP[c]	—	—	2.0	>100

[a] IC_{50}: 50% inhibitory concentration (μM). [b] CC_{50}: 50% cytotoxic concentration (μM). [c] HRP: peptide mimics of heptad repeat domain in the MERS spike protein, which is responsible for conformational change during spike protein-mediated viral–host membrane fusion.

Table 2 Inhibitory activity of **1h–1u** against MERS-S pseudovirus

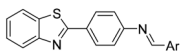

Compound	Ar	IC_{50}[a]	CC_{50}[b]
1h		0.57 ± 0.11	>100
1i		0.52 ± 0.03	>100
1j		0.20 ± 0.05	>100
1k		0.40 ± 0.01	>100
1l		0.22 ± 0.03	>100
1m		0.34 ± 0.24	>100
1n		>10.00	>100
1o		0.14 ± 0.06	>100
1p		>10.00	>100
1q		6.52 ± 1.14	>100
1r		0.62 ± 0.31	>100
1s		>10.00	>100
1t		8.80 ± 0.01	>100
1u		>10.00	>100
HRP[c]	—	2.00	>100

[a] IC_{50}: 50% inhibitory concentration (μM). [b] CC_{50}: 50% cytotoxic concentration (μM). [c] HRP: peptide mimics of heptad repeat domain in the MERS spike protein, which is responsible for conformational change during spike protein-mediated viral–host membrane fusion.

Open Access Article. Published on 07 2020. Downloaded on 2025/12/13 4:57:53.
This article is licensed under a Creative Commons Attribution-NonCommercial 3.0 Unported Licence.

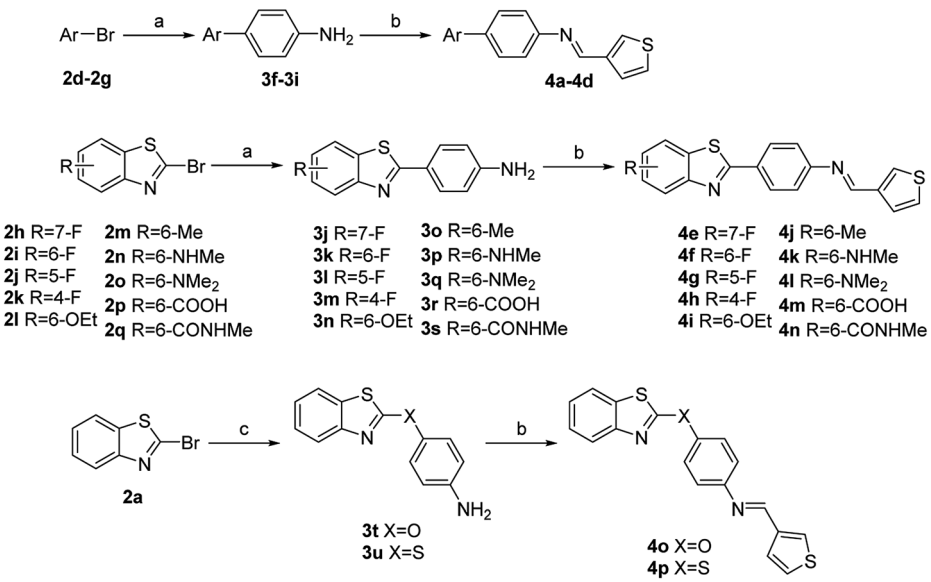

Scheme 2 Reagents and conditions. (a) 4-Aminophenylboronic acid pinacol ester, $Pd(dppf)Cl_2 \cdot CH_2Cl_2$, K_2CO_3, DMF, 70 °C, 16 h. (b) Thiophene-3-carbaldehyde, AcOH, MeOH, reflux, 2 h. (c) For **4o**: 4-aminophenol, *t*-BuONa, K_2CO_3, DMF, room temperature, 5 h; for **4p**: 4-aminobenzenethiol, K_2CO_3, MeCN, reflux, 3 h.

Table 3 Inhibitory activity of **4a–4p** against MERS-S pseudovirus

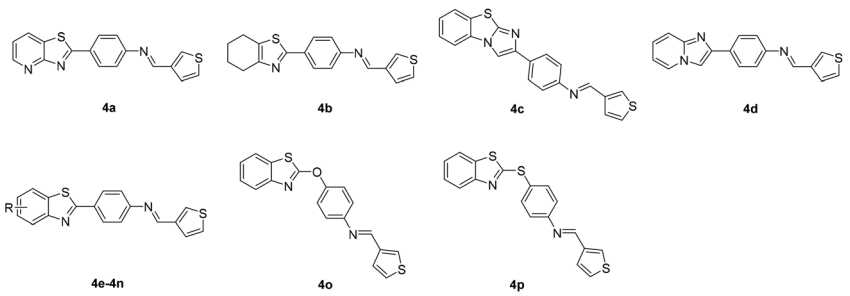

Compound	R	IC_{50}[a]	CC_{50}[b]
4a	—	>10.00	>100
4b	—	>10.00	>100
4c	—	>10.00	>100
4d	—	>10.00	>100
4e	7-F	1.67 ± 0.30	>100
4f	6-F	0.09 ± 0.01	>100
4g	5-F	1.00 ± 0.07	>100
4h	4-F	0.53 ± 0.02	>100
4i	6-OEt	>10.00	>100
4j	6-Me	>10.00	>100
4k	6-NHMe	>10.00	>100
4l	6-NMe_2	>10.00	>100
4m	6-COOH	>10.00	>100
4n	6-CONHMe	>10.00	>100
4o	—	>10.00	>100
4p	—	>10.00	>100
HRP[c]	—	2.00	>100

[a] IC_{50}: 50% inhibitory concentration (μM). [b] CC_{50}: 50% cytotoxic concentration (μM). [c] HRP: peptide mimics of heptad repeat domain in the MERS spike protein, which is responsible for conformational change during spike protein-mediated viral–host membrane fusion.

 This journal is © The Royal Society of Chemistry 2020

Open Access Article. Published on 07 2020. Downloaded on 2025/12/13 4:57:53.
This article is licensed under a Creative Commons Attribution-NonCommercial 3.0 Unported Licence.

a phenyl group B (**1e**) in the linker region. Modest inhibitory activity was evident when the phenyl group B was replaced with a pyridyl group (**1d**). When the imine portion was reduced or replaced with amide (**1f** and **1g**), inhibitory activity was markedly reduced. Modification was then focused on the phenyl ring C of the compound, and derivatives **1h–1m** were designed and synthesized in a similar way as **1a**. Their IC_{50} values on MERS-S pseudovirus and CC_{50} values are summarized in Table 2.

All the derivatives demonstrated inhibitory activities with IC_{50} values ranging from 0.20 μM to 0.57 μM, and no cell toxicity. Either changing the position of the hydroxyl group and methoxy group or the absence of these groups increased the activity slightly, the compounds containing 3-OH were more potent. Changing the phenyl ring C to a pyridine ring did not elicit significant changes in inhibitory activity.

Given the results of **1h–1m**, further structural extensions were investigated in the phenyl ring C area. A series of five-member aromatic heterocycles were introduced to replace the phenyl ring C. Derivatives **1o** and **1r**, substituted by a 3-thienyl group, exhibited marked inhibitory activity with respective IC_{50} values of 0.14 μM and 0.62 μM. The introduction of a nitro group on the thiophene motif caused a slight reduction in inhibitory activity. Compound **1q** exhibited modest inhibitory capacity, indicating that the substitution mode influenced activity. None of the compounds in this series exhibited any cytotoxicity.

Based on the above results, while retaining the 3-thienyl group at ring C position a structure–activity relationship investigation was conducted in which structural extensions at the benzothiazole part of this compound were assessed. As shown in Scheme 2, commercially available aryl bromides were used as starting materials, and the corresponding intermediate amines **3f–3u** were prepared using Suzuki–Miyaura cross-coupling or a nucleophilic substitution reaction. The final compounds **4a–4p** were readily generated *via* a similar method that has been previously outlined in Scheme 1. Their IC_{50} values against MERS-S pseudovirus and their CC_{50} values are summarized in Table 3.

Replacement of a benzothiazole unit (**4a–4d**) abolished the inhibitory activity (Table 3), further confirming that the benzothiazole motif played a pivotal role in inhibitory capacity. An atom of fluorine—the most electronegative of the halogens—was then introduced at different benzothiazole positions, and the derivatives obtained (**4e–4h**) exhibited diverse inhibitory capacity. Introduction of a fluorine atom at the 6-position of the phenyl ring A (**4f**) increased inhibition activity, with an IC_{50} value of 0.09 μM, and introduction of a fluorine atom at another position resulted in modest inhibitory potency. The introduction of other groups such as alkoxy, alkyl, amino, and carboxyl groups (**4i–4n**) reduced inhibitory activity. The reduction in inhibitory capacity is most likely due to the steric effect of the bulky group. To increase the flexibility of the compounds, heteroatom was introduced between the benzothiazole group and phenyl ring B to obtain **4o** and **4p**, but unfortunately inhibitory activity was abolished. The CC_{50} values of these compounds were greater than 100 μM, indicating no toxicity or at least lower toxicity to uninfected cells. The results of the study suggest that compound **4f** has potential for the subsequent development of novel anti-MERS-CoV agents.

Conclusion

In summary, a series of new 1-phenyl-*N*-(benzothiazol-2-yl) methanimine derivatives was developed as MERS-CoV entry inhibitors *via* modification of a hit compound, which was obtained by screening an orthogonal cocktail library composed of 48 000 compounds. All of the compounds were assessed for their capacity to inhibit the entry of pseudovirus expressing MERS-CoV S protein. Structure–activity relationships indicated that benzothiazole was the best option for region A of the structure, and the presence of a phenyl ring B and an imine portion favored the retention of inhibitory activity against MERS-CoV. The introduction of a 6-member aromatic ring or a 3-thiophene ring at ring C position also favored inhibitory activity. Remarkably, compound **4f**, with an IC_{50} value of 0.09 μM, was more potent than the initial hit compound. In addition, none of these types of structures exhibited cytotoxicity. The present study demonstrates an approach for the structural modification of hit compounds, and a novel skeleton for new anti-MERS-CoV drug research. Further research on this series of derivatives is ongoing.

Experimental

Chemistry

Commercial reagents and solvents were purchased commercial suppliers and used without further purification. All non-aqueous reactions were under a nitrogen atmosphere and all non-aqueous reaction vessels were oven-dried. Flash column chromatography was performed using Qingdao Ocean silica gel (200–300) with the indicated eluents. All final compounds were characterized by their NMR and HRMS spectra, unless stated otherwise. ^{1}H NMR spectra were recorded at a spectrometer frequency of 400 MHz, and ^{13}C NMR spectra at 100 MHz on Bruker Avance 400. Chemical shifts are reported in δ (ppm) using signals of tetramethylsilane (TMS) as the internal standard. High-resolution mass spectra (HRMS) were measured on a Bruker ESI-TOF high-resolution mass spectrometer. Melting points (mp) were uncorrected and were recorded on a Buchi B-54 melting point apparatus.

General procedure for the synthesis of compounds 3a–3d and 3f–3s

2a–2q (1 mmol), the corresponding pinacol borate (1.2 mmol) and Pd(dppf)$Cl_2 \cdot CH_2Cl_2$ (0.05 mmol) were suspended in DMF (6 mL) in the presence of 2 M K_2CO_3 (2 mL) and stirred at 70 °C overnight under nitrogen. The reaction mixture was diluted with H_2O (40 mL) and organics were extracted with EtOAc (3× 30 mL). The combined organic layers were washed with brine (30 mL), dried over $MgSO_4$, filtered and concentrated *in vacuo* to afford crude mixture. The crude mixture was then purified by flash column chromatography in a mixture of petroleum ether and ethyl acetate to yield the pure products **3a–3d** and **3f–3s**.

Open Access Article. Published on 07 2020. Downloaded on 2025/12/13 4:57:53.
This article is licensed under a Creative Commons Attribution-NonCommercial 3.0 Unported Licence.

4-(Benzo[*d*]thiazol-2-yl)aniline (3a). Yellow solid; yield 60%. ^{1}H NMR (400 MHz, DMSO-d_6) δ 8.01 (d, J = 7.9 Hz, 1H, ArH), 7.89 (d, J = 8.1 Hz, 1H, ArH), 7.76 (d, J = 8.4 Hz, 2H, ArH), 7.48–7.42 (m, 1H, ArH), 7.37–7.31 (m, 1H, ArH), 6.67 (d, J = 8.4 Hz, 2H, ArH), 5.88 (s, 2H, NH_2). ^{13}C NMR (100 MHz, chloroform-d) δ 168.5, 154.3, 149.2, 134.7, 129.2, 126.1, 124.4, 124.0, 122.6, 121.4, 114.7.

4-(Benzo[*d*]oxazol-2-yl)aniline (3b). Light orange solid; yield 65%. ^{1}H NMR (400 MHz, DMSO-d_6) δ 7.86 (d, J = 8.3 Hz, 2H, ArH), 7.70–7.63 (m, 2H, ArH), 7.36–7.27 (m, 2H, ArH), 6.70 (d, J = 8.4 Hz, 2H, ArH), 5.96 (s, 2H, NH_2). ^{13}C NMR (100 MHz, DMSO-d_6) δ 163.6, 152.5, 149.8, 142.1, 128.9 (2C), 124.3, 124.0, 118.7, 113.5 (2C), 112.7, 110.2.

4-(1*H*-Benzo[*d*]imidazol-2-yl)aniline (3c). Light orange solid; yield 70%. ^{1}H NMR (400 MHz, DMSO-d_6) δ 12.43 (s, 1H, imidazole), 7.87 (d, J = 8.2 Hz, 2H, ArH), 7.49 (s, 2H, ArH), 7.14–7.10 (m, 2H, ArH), 6.69 (d, J = 8.2 Hz, 2H, ArH), 5.58 (s, 2H, NH_2). ^{13}C NMR (100 MHz, DMSO-d_6) δ 152.6, 150.5, 127.7 (2C), 121.2, 117.3, 113.5 (2C).

6-(Benzo[*d*]thiazol-2-yl)pyridin-3-amine (3d). Yellow solid; yield 70%. This intermediate is used directly in the next step without further purification.

4-(Thiazolo[4,5-*b*]pyridin-2-yl)aniline (3f). Yellow solid; yield 24%. ^{1}H NMR (400 MHz, chloroform-d) δ 8.66 (d, J = 3.6 Hz, 1H, ArH), 8.17 (d, J = 7.9 Hz, 1H, ArH), 8.00 (d, J = 8.4 Hz, 2H, ArH), 7.25–7.21 (m, 1H, ArH), 6.74 (d, J = 8.6 Hz, 2H, ArH), 4.09 (s, 2H, NH_2).

4-(4,5,6,7-Tetrahydrobenzo[*d*]thiazol-2-yl)aniline (3g). Light yellow solid; yield 62%. ^{1}H NMR (400 MHz, chloroform-d) δ 7.68 (d, J = 8.6 Hz, 2H, ArH), 6.67 (d, J = 8.5 Hz, 2H, ArH), 3.84 (s, 2H, NH_2), 2.83–2.75 (m, 4H, CH_2), 1.91–1.81 (m, 4H, CH_2). ^{13}C NMR (100 MHz, chloroform-d) δ 164.2, 149.7, 146.8, 126.6 (2C), 126.3, 123.9, 113.8 (2C), 25.9, 22.6, 22.4, 22.1.

4-(Benzo[*d*]imidazo[2,1-*b*]thiazol-2-yl)aniline (3h). Light yellow solid; yield 45%. ^{1}H NMR (400 MHz, chloroform-d) δ 7.82 (s, 1H, ArH), 7.70–7.65 (m, 3H, ArH), 7.57 (d, J = 8.0 Hz, 1H, ArH), 7.46–7.40 (m, 1H, ArH), 7.34–7.28 (m, 1H, ArH), 6.74 (d, J = 8.4 Hz, 2H, ArH), 3.74 (s, 2H, NH_2). ^{13}C NMR (100 MHz, chloroform-d) δ 147.1, 146.7, 145.0, 131.3, 129.2, 125.4 (2C), 125.1, 123.6, 123.5, 123.3, 114.3 (2C), 111.4, 104.2.

4-(Imidazo[1,2-*a*]pyridin-2-yl)aniline (3i). Yellow solid; yield 56%. ^{1}H NMR (400 MHz, chloroform-d) δ 8.07 (d, J = 6.7 Hz, 1H, ArH), 7.76 (d, J = 8.5 Hz, 2H, ArH), 7.73 (s, 1H, ArH), 7.59 (d, J = 9.1 Hz, 1H, ArH), 7.15–7.09 (m, 1H, ArH), 6.77–6.70 (m, 3H, ArH), 3.75 (s, 2H, NH_2). ^{13}C NMR (100 MHz, chloroform-d) δ 145.4, 145.3, 144.5, 126.2 (2C), 124.3, 123.3, 123.2, 116.2, 114.2 (2C), 111.0, 105.7.

4-(7-Fluorobenzo[*d*]thiazol-2-yl)aniline (3j). Yellow solid; yield 69%. ^{1}H NMR (400 MHz, DMSO-d_6) δ 7.80–7.73 (m, 3H, ArH), 7.50–7.42 (m, 1H, ArH), 7.24–7.18 (m, 1H, ArH), 6.69 (d, J = 8.3 Hz, 2H, ArH), 6.04 (s, 2H, NH_2). ^{13}C NMR (100 MHz, DMSO-d_6) δ 169.0 (d, J = 1.5 Hz), 156.8 (d, J = 2.5 Hz), 156.3 (d, J = 246.1 Hz), 152.6, 129.1 (2C), 127.5 (d, J = 7.5 Hz), 120.1 (d, J = 16.2 Hz), 119.2, 118.0 (d, J = 3.3 Hz), 113.6 (2C), 109.9 (d, J = 18.7 Hz).

4-(6-Fluorobenzo[*d*]thiazol-2-yl)aniline (3k). White solid; yield 71%. ^{1}H NMR (400 MHz, chloroform-d) δ 7.94–7.90 (m, 1H, ArH), 7.85 (d, J = 7.8 Hz, 2H, ArH), 7.52 (d, J = 8.1 Hz, 1H, ArH), 7.20–7.14 (m, 1H, ArH), 6.73 (d, J = 8.9 Hz, 2H, ArH), 4.02 (s, 2H, NH_2). ^{13}C NMR (100 MHz, chloroform-d) δ 167.2 (d, J = 3.2 Hz), 159.0 (d, J = 244.5 Hz), 149.8 (d, J = 1.8 Hz), 148.2, 134.5 (d, J = 11.1 Hz), 128.0 (2C), 122.6, 122.2 (d, J = 9.2 Hz), 113.8 (2C), 113.5 (d, J = 24.5 Hz), 106.7 (d, J = 26.7 Hz).

4-(5-Fluorobenzo[*d*]thiazol-2-yl)aniline (3l). White solid; yield 59%. ^{1}H NMR (400 MHz, DMSO-d_6) δ 8.01 (dd, J = 8.8, 5.4 Hz, 1H, ArH), 7.76 (d, J = 8.5 Hz, 2H, ArH), 7.72 (dd, J = 10.0, 2.6 Hz, 1H, ArH), 7.25–7.17 (m, 1H, ArH), 6.68 (d, J = 8.5 Hz, 2H, ArH), 5.98 (s, 2H, NH_2). ^{13}C NMR (100 MHz, DMSO-d_6) δ 170.9, 161.3 (d, J = 240.0 Hz), 154.8 (d, J = 12.3 Hz), 152.4, 129.4 (d, J = 2.0 Hz), 128.8 (2C), 122.9 (d, J = 9.9 Hz), 119.8, 113.5 (2C), 112.3 (d, J = 24.7 Hz), 107.8 (d, J = 23.6 Hz).

4-(4-Fluorobenzo[*d*]thiazol-2-yl)aniline (3m). White solid; yield 61%. ^{1}H NMR (400 MHz, DMSO-d_6) δ 7.85 (dd, J = 7.6, 1.4 Hz, 1H, ArH), 7.77 (d, J = 8.6 Hz, 2H, ArH), 7.37–7.28 (m, 2H, ArH), 6.67 (d, J = 8.7 Hz, 2H, ArH), 5.99 (s, 2H, NH_2). ^{13}C NMR (100 MHz, DMSO-d_6) δ 169.0, 154.3 (d, J = 252.5 Hz), 152.5, 142.2 (d, J = 13.2 Hz), 136.5 (d, J = 3.9 Hz), 129.0 (2C), 125.1 (d, J = 7.1 Hz), 119.5, 118.0 (d, J = 4.0 Hz), 113.5 (2C), 111.9 (d, J = 17.7 Hz).

4-(6-Ethoxybenzo[*d*]thiazol-2-yl)aniline (3n). Brown solid; yield 38%. ^{1}H NMR (400 MHz, chloroform-d) δ 7.88–7.82 (m, 3H, ArH), 7.31 (s, 1H, ArH), 7.04 (d, J = 8.9 Hz, 1H, ArH), 6.73 (d, J = 8.1 Hz, 2H, ArH), 4.09 (q, J = 6.8 Hz, 2H, CH_2), 3.96 (s, 2H, NH_2), 1.45 (t, J = 6.9 Hz, 3H, CH_3). ^{13}C NMR (100 MHz, chloroform-d) δ 166.0, 156.6, 148.8, 148.7, 135.8, 128.8 (2C), 124.2, 122.9, 115.5, 114.8 (2C), 105.0, 64.1, 14.9.

4-(6-Methylbenzo[*d*]thiazol-2-yl)aniline (3o). Yellow solid; yield 60%. ^{1}H NMR (400 MHz, chloroform-d) δ 7.90–7.85 (m, 3H, ArH), 7.64 (s, 1H, ArH), 7.26–7.22 (m, 1H, ArH), 6.73 (d, J = 8.5 Hz, 2H, ArH), 3.97 (s, 2H, NH_2), 2.48 (s, 3H, CH_3). ^{13}C NMR (100 MHz, chloroform-d) δ 166.1, 151.2, 142.9, 134.2, 134.0, 128.1, 127.8, 127.6, 126.3, 121.3, 118.9, 21.1.

2-(4-Aminophenyl)-*N*-methylbenzo[*d*]thiazol-6-amine (3p). Orange solid; yield 70%. ^{1}H NMR (400 MHz, chloroform-d) δ 7.82 (d, J = 8.5 Hz, 2H, ArH), 7.77 (d, J = 8.7 Hz, 1H, ArH), 6.98 (s, 1H, ArH), 6.77–6.70 (m, 3H, ArH), 3.91 (s, 2H, NH_2), 2.90 (s, 3H, CH_3). ^{13}C NMR (100 MHz, chloroform-d) δ 162.7, 147.4, 146.0, 145.8, 135.7, 127.5 (2C), 123.6, 121.8, 113.8 (2C), 113.0, 100.8, 30.0.

2-(4-Aminophenyl)-*N*,*N*-dimethylbenzo[*d*]thiazol-6-amine (3q). Orange solid; yield 72%. ^{1}H NMR (400 MHz, chloroform-d) δ 7.85–7.81 (m, 3H, ArH), 7.10 (s, 1H, ArH), 6.93 (dd, J = 9.0, 2.5 Hz, 1H, ArH), 6.72 (d, J = 8.6 Hz, 2H, ArH), 3.92 (s, 2H, NH_2), 3.02 (s, 6H, CH_3). ^{13}C NMR (100 MHz, chloroform-d) δ 163.9, 148.5, 148.5, 146.2, 136.6, 128.6 (2C), 124.6, 122.5, 114.8 (2C), 113.2, 103.3, 41.2.

2-(4-Aminophenyl)benzo[*d*]thiazole-6-carboxylic acid (3r). Yellow solid; yield 60%. ^{1}H NMR (400 MHz, DMSO-d_6) δ 12.99 (br, 1H, COOH), 8.62 (s, 1H, ArH), 8.00 (d, J = 8.5 Hz, 1H, ArH), 7.93 (d, J = 8.6 Hz, 1H, ArH), 7.79 (d, J = 8.3 Hz, 2H, ArH), 6.67 (d, J = 8.3 Hz, 2H, ArH), 6.04 (s, 2H, NH_2). ^{13}C NMR (100 MHz,

Open Access Article. Published on 07 2020. Downloaded on 2025/12/13 4:57:53.
This article is licensed under a Creative Commons Attribution-NonCommercial 3.0 Unported Licence.

DMSO-d_6) δ 171.7, 167.0, 156.8, 152.7, 133.8, 129.1 (2C), 127.3, 126.3, 123.8, 121.3, 119.6, 113.5 (2C).

2-(4-Aminophenyl)-*N*-methylbenzo[*d*]thiazole-6-carboxamide (3s). Light yellow solid; yield 47%. ^{1}H NMR (400 MHz, DMSO-d_6) δ 8.51 (q, J = 4.2 Hz, 1H, –(C=O)NH–), 8.48 (s, 1H, ArH), 7.95–7.88 (m, 2H, ArH), 7.79 (d, J = 8.4 Hz, 2H, ArH), 6.68 (d, J = 8.6 Hz, 2H, ArH), 5.99 (s, 2H, NH_2), 2.82 (d, J = 4.4 Hz, 3H, CH_3). ^{13}C NMR (100 MHz, DMSO-d_6) δ 170.4, 166.1, 155.6, 152.5, 133.6, 130.4, 129.0 (2C), 125.3, 121.1, 121.1, 119.7, 113.5 (2C), 26.4.

Synthesis of 4-(benzo[*d*]thiazol-2-yloxy)aniline (3t)

4-Aminophenol (2 mmol) was dissolved in DMF (5 mL) followed by the addition of *t*-BuONa (2.4 mmol) and stirred at room temperature for 1 h. Then **2a** (2 mmol) and K_2CO_3 (2.4 mmol) were added and stirred for another 4 h. The reaction mixture was diluted with H_2O (40 mL) and organics were extracted with EtOAc (3× 30 mL). The combined organic layers were washed with brine (30 mL), dried over $MgSO_4$, filtered and concentrated *in vacuo* to afford crude mixture. The crude mixture was then purified by flash column chromatography in a mixture of petroleum ether and ethyl acetate to yield the pure product **3t**. Yellow oil, yield 80%. ^{1}H NMR (400 MHz, chloroform-*d*) δ 7.73 (d, J = 8.1 Hz, 1H, ArH), 7.63 (d, J = 8.0 Hz, 1H, ArH), 7.40–7.34 (m, 1H, ArH), 7.25–7.21 (m, 1H, ArH), 7.12 (d, J = 8.7 Hz, 2H, ArH), 6.71 (d, J = 8.7 Hz, 2H, ArH), 3.74 (s, 2H, NH_2). ^{13}C NMR (100 MHz, chloroform-*d*) δ 173.6, 149.4, 147.2, 145.0, 132.2, 126.2, 123.8, 121.8 (2C), 121.6, 121.3, 115.9 (2C).

Synthesis of 4-(benzo[*d*]thiazol-2-ylthio)aniline (3u)

4-Aminobenzenethiol (2 mmol) and **2a** (2 mmol) was dissolved in MeCN (5 mL) followed by the addition of K_2CO_3 (2.4 mmol) and stirred at reflux for 3 h. Upon completion, the reaction was allowed to cold to room temperature. The reaction mixture was diluted with H_2O (40 mL) and organics were extracted with EtOAc (3× 30 mL). The combined organic layers were washed with brine (30 mL), dried over $MgSO_4$, filtered and concentrated *in vacuo* to afford crude mixture. The crude mixture was then purified by flash column chromatography in a mixture of petroleum ether and ethyl acetate to yield the pure product **3u**. White solid; yield 50%. ^{1}H NMR (400 MHz, chloroform-*d*) δ 7.84 (d, J = 8.2 Hz, 1H, ArH), 7.62 (d, J = 8.0 Hz, 1H, ArH), 7.50 (d, J = 8.4 Hz, 2H, ArH), 7.41–7.35 (m, 1H, ArH), 7.25–7.19 (m, 1H, ArH), 6.74 (d, J = 8.4 Hz, 2H, ArH), 4.02 (s, 2H, NH_2). ^{13}C NMR (100 MHz, chloroform-*d*) δ 172.4, 153.3, 148.0, 136.6 (2C), 134.4, 125.0, 122.8, 120.6, 119.7, 115.6, 114.9 (2C).

General procedure for the synthesis of compounds 1a–1d, 1h–1u and 4a–4p

The catalytic amount of acetic acid was added to a solution of **3a–3d**, **3f–3u** (0.44 mmol) and the corresponding aromatic aldehyde (0.53 mmol) in MeOH (4 mL), the mixture was stirred at reflux for 2 h. The resulting precipitate was isolated by suction filtration and washed with MeOH (8 mL) to give the pure products **1a–1d**, **1h–1u** and **4a–4p**.

(*E*)-2-(((4-(Benzo[*d*]thiazol-2-yl)phenyl)imino)methyl)-6-methoxyphenol (1a). Orange solid; yield 63%. Mp 175–176 °C. ^{1}H NMR (400 MHz, chloroform-*d*) δ 13.44 (s, 1H, OH), 8.67 (s, 1H, –CH=N–), 8.14 (d, J = 8.2 Hz, 2H, ArH), 8.07 (d, J = 8.2 Hz, 1H, ArH), 7.90 (d, J = 7.9 Hz, 1H, ArH), 7.52–7.48 (m, 1H, ArH), 7.41–7.36 (m, 3H, ArH), 7.06–6.99 (m, 2H, ArH), 6.93–6.87 (m, 1H, ArH), 3.94 (s, 3H, CH_3). ^{13}C NMR (100 MHz, chloroform-*d*) δ 166.1, 162.3, 153.1, 150.5, 149.3, 147.5, 134.0, 131.2, 127.7, 125.4, 124.2, 123.0, 122.2, 120.8, 120.6, 118.0, 117.7, 114.2, 55.2. HRMS (ESI) *m*/*z*: calculated for $C_{21}H_{16}N_2NaO_2S$ $[M + Na]^+$: 383.0825, found: 383.0823.

(*E*)-2-(((4-(Benzo[*d*]oxazol-2-yl)phenyl)imino)methyl)-6-methoxyphenol (1b). Orange solid; yield 55%. Mp 218–219 °C. ^{1}H NMR (400 MHz, chloroform-*d*) δ 13.35 (s, 1H, OH), 8.69 (s, 1H, –CH=N–), 8.31 (d, J = 8.3 Hz, 2H, ArH), 7.80–7.76 (m, 1H, ArH), 7.61–7.57 (m, 1H, ArH), 7.42 (d, J = 8.2 Hz, 2H, ArH), 7.38–7.34 (m, 2H, ArH), 7.06–7.01 (m, 2H, ArH), 6.94–6.88 (m, 1H, ArH), 3.95 (s, 3H, CH_3). ^{13}C NMR (100 MHz, chloroform-*d*) δ 162.7, 161.5, 150.6, 149.9, 149.8, 147.5, 141.2, 127.9 (2C), 124.6, 124.2, 123.7, 123.0, 120.8 (2C), 119.0, 118.0, 117.8, 114.3, 109.6, 55.2. HRMS (ESI) *m*/*z*: calculated for $C_{21}H_{16}N_2NaO_3$ $[M + Na]^+$: 367.1053, found: 367.1041.

(*E*)-2-(((4-(1*H*-Benzo[*d*]imidazol-2-yl)phenyl)imino)methyl)-6-methoxyphenol (1c). Red solid; yield 36%. Mp > 220 °C. ^{1}H NMR (400 MHz, DMSO-d_6) δ 13.10 (s, 1H, OH), 12.94 (s, 1H, imidazole), 9.06 (s, 1H, –CH=N–), 8.27 (d, J = 8.2 Hz, 2H, ArH), 7.68 (d, J = 7.5 Hz, 1H, ArH), 7.60 (d, J = 8.2 Hz, 2H, ArH), 7.54 (d, J = 7.5 Hz, 1H, ArH), 7.28 (d, J = 7.5 Hz, 1H, ArH), 7.23–7.20 (m, 2H, ArH), 7.15 (d, J = 7.7 Hz, 1H, ArH), 6.95–6.91 (m, 1H, ArH), 3.84 (s, 3H, CH_3). ^{13}C NMR (100 MHz, DMSO-d_6) δ 163.9, 150.7, 150.6, 149.0, 147.9, 143.9, 135.0, 128.6, 127.6 (2C), 123.9, 122.6, 122.0 (2C), 121.7, 119.3, 118.8, 118.7, 115.8, 111.3, 55.9. HRMS (ESI) *m*/*z*: calculated for $C_{21}H_{17}N_3NaO_2$ $[M + Na]^+$: 366.1213, found: 366.1198.

(*E*)-2-(((6-(Benzo[*d*]thiazol-2-yl)pyridin-3-yl)imino)methyl)-6-methoxyphenol (1d). Yellow solid; yield 64%. Mp > 220 °C. ^{1}H NMR (400 MHz, chloroform-*d*) δ 13.00 (s, 1H, OH), 8.71 (s, 1H, –CH=N–), 8.61 (d, J = 2.4 Hz, 1H, ArH), 8.43 (d, J = 8.4 Hz, 1H, ArH), 8.09 (d, J = 8.2 Hz, 1H, ArH), 7.96 (d, J = 8.0 Hz, 1H, ArH), 7.74 (dd, J = 8.4, 2.5 Hz, 1H, ArH), 7.54–7.49 (m, 1H, ArH), 7.44–7.41 (m, 1H, ArH), 7.09–7.03 (m, 2H, ArH), 6.96–6.90 (m, 1H, ArH), 3.95 (s, 3H, CH_3). ^{13}C NMR (100 MHz, chloroform-*d*) δ 167.5, 163.8, 153.3, 150.4, 148.7, 147.5, 144.6, 142.3, 135.2, 127.6, 125.3, 124.7, 123.2, 122.5, 121.0, 120.3, 118.1, 117.9, 114.7, 55.2. HRMS (ESI) *m*/*z*: calculated for $C_{20}H_{15}N_3NaO_2S$ $[M + Na]^+$: 384.0777, found: 384.0786.

(*E*)-*N*-(4-(Benzo[*d*]thiazol-2-yl)phenyl)-1-phenylmethanimine (1h). Yellow solid; yield 22%. Mp 200–202 °C. ^{1}H NMR (400 MHz, chloroform-*d*) δ 8.51 (s, 1H, –CH=N–), 8.14 (d, J = 8.5 Hz, 2H, ArH), 8.08 (d, J = 8.2 Hz, 1H, ArH), 7.96–7.93 (m, 2H, ArH), 7.91 (d, J = 8.0 Hz, 1H, ArH), 7.52–7.47 (m, 4H, ArH), 7.41–7.36 (m, 1H, ArH), 7.32 (d, J = 8.4 Hz, 2H, ArH). ^{13}C NMR (100 MHz, chloroform-*d*) δ 166.6, 160.1, 153.4, 153.2, 134.9, 134.0, 130.8, 130.2, 128.0 (2C), 127.8 (2C), 127.6 (2C), 125.3, 124.1, 122.1, 120.6, 120.5 (2C). HRMS (ESI) *m*/*z*: calculated for $C_{20}H_{14}N_2NaS$ $[M + Na]^+$: 337.0770, found: 337.0752.

Open Access Article. Published on 07 2020. Downloaded on 2025/12/13 4:57:53.
This article is licensed under a Creative Commons Attribution-NonCommercial 3.0 Unported Licence.

(*E*)-2-(((4-(Benzo[*d*]thiazol-2-yl)phenyl)imino)methyl)phenol (1i). Light yellow solid; yield 60%. Mp 205–207 °C. ^{1}H NMR (400 MHz, DMSO-d_6) δ 12.81 (s, 1H, OH), 9.06 (s, 1H, –CH=N–), 8.19–8.17 (m, 3H, ArH), 8.07 (d, J = 8.1 Hz, 1H, ArH), 7.71 (d, J = 7.5 Hz, 1H, ArH), 7.60 (d, J = 8.4 Hz, 2H, ArH), 7.58–7.54 (m, 1H, ArH), 7.47–7.44 (m, 2H, ArH), 7.03–6.99 (m, 2H, ArH). ^{13}C NMR (100 MHz, DMSO-d_6) δ 166.6, 164.3, 160.3, 153.6, 150.7, 134.5, 133.7, 132.6, 131.1, 128.4 (2C), 126.7, 125.5, 122.8, 122.4 (2C), 122.3, 119.3, 119.3, 116.7. HRMS (ESI) *m*/*z*: calculated for $C_{20}H_{15}N_2OS$ $[M + H]^+$: 331.0900, found: 331.0902.

(*E*)-*N*-(4-(Benzo[*d*]thiazol-2-yl)phenyl)-1-(3-methoxyphenyl) methanimine (1j). Light yellow solid; yield 45%. Mp 118–119 °C. ^{1}H NMR (400 MHz, DMSO-d_6) δ 8.67 (s, 1H, –CH=N–), 8.15–8.13 (m, 3H, ArH), 8.06 (d, J = 8.1 Hz, 1H, ArH), 7.57–7.54 (m, 3H, ArH), 7.48–7.42 (m, 4H, ArH), 7.14 (d, J = 8.2 Hz, 1H, ArH), 3.84 (s, 3H, CH_3). ^{13}C NMR (100 MHz, DMSO-d_6) δ 166.8, 161.8, 159.5, 153.8, 153.6, 137.2, 134.4, 130.4, 130.0, 128.3 (2C), 126.6, 125.4, 122.7, 122.3, 122.0 (2C), 121.9, 118.1, 112.7, 55.2. HRMS (ESI) *m*/*z*: calculated for $C_{21}H_{17}N_2NaOS$ $[M + H]^+$: 345.1056, found: 345.1071.

(*E*)-3-(((4-(Benzo[*d*]thiazol-2-yl)phenyl)imino)methyl) benzene-1,2-diol (1k). Red solid; yield 26%. Mp > 220 °C. ^{1}H NMR (400 MHz, DMSO-d_6) δ 9.01 (s, 1H, –CH=N–), 8.19–8.13 (m, 3H, ArH), 8.07 (d, J = 8.1 Hz, 1H, ArH), 7.59 (d, J = 8.2 Hz, 2H, ArH), 7.57–7.54 (m, 1H, ArH), 7.49–7.45 (m, 1H, ArH), 7.15 (d, J = 6.9 Hz, 1H, ArH), 6.99 (d, J = 6.8 Hz, 1H, ArH), 6.84–6.80 (m,1H, ArH). ^{13}C NMR (100 MHz, DMSO-d_6) δ 166.6, 164.7, 153.6, 150.5, 149.4, 145.6, 134.5, 131.1, 128.4 (2C), 126.7, 125.5, 122.9, 122.8, 122.4 (2C), 122.3, 119.4, 119.3, 118.9. HRMS (ESI) *m*/*z*: calculated for $C_{20}H_{14}N_2NaO_2S$ $[M + Na]^+$: 369.0668, found: 369.0654.

(*E*)-5-(((4-(Benzo[*d*]thiazol-2-yl)phenyl)imino)methyl)-2-methoxyphenol (1l). Yellow solid; yield 54%. Mp 214–215 °C. ^{1}H NMR (400 MHz, DMSO-d_6) δ 9.40 (br, 1H, OH), 8.52 (s, 1H, –CH=N–), 8.14–8.12 (m, 3H, ArH), 8.05 (d, J = 8.1 Hz, 1H, ArH), 7.57–7.52 (m, 1H, ArH), 7.47–7.44 (m, 2H, ArH), 7.39–7.35 (m, 3H, ArH), 7.06 (d, J = 8.3 Hz, 1H, ArH), 3.85 (s, 3H, CH_3). ^{13}C NMR (100 MHz, DMSO-d_6) δ 166.9, 161.3, 154.3, 153.6, 151.3, 146.8, 134.4, 129.9, 128.9, 128.2 (2C), 126.6, 125.4, 122.9, 122.7, 122.3, 121.9 (2C), 113.7, 111.6, 55.6. HRMS (ESI) *m*/*z*: calculated for $C_{21}H_{17}N_2O_2S$ $[M + H]^+$: 361.1005, found: 361.0986.

(*E*)-*N*-(4-(Benzo[*d*]thiazol-2-yl)phenyl)-1-(pyridin-3-yl) methanimine (1m). Yellow solid; yield 17%. Mp 151–153 °C. ^{1}H NMR (400 MHz, chloroform-*d*) δ 9.05 (s, 1H, –CH=N–), 8.73 (d, J = 4.7 Hz, 1H, ArH), 8.55 (s, 1H, ArH), 8.32 (d, J = 8.0 Hz, 1H, ArH), 8.15 (d, J = 8.1 Hz, 2H, ArH), 8.08 (d, J = 8.2 Hz, 1H, ArH), 7.91 (d, J = 8.0 Hz, 1H, ArH), 7.52–7.48 (m, 1H, ArH), 7.46–7.42 (m, 1H, ArH), 7.41–7.37 (m, 1H, ArH), 7.33 (d, J = 8.1 Hz, 2H, ArH). ^{13}C NMR (100 MHz, chloroform-*d*) δ 167.3, 158.0, 154.2, 153.6, 152.3, 151.1, 135.1, 135.0, 131.8, 131.6, 128.6 (2C), 126.4, 125.2, 123.9, 123.2, 121.6, 121.5 (2C). HRMS (ESI) *m*/*z*: calculated for $C_{19}H_{14}N_3S$ $[M + H]^+$: 316.0903, found: 316.0893.

(*E*)-*N*-(4-(Benzo[*d*]thiazol-2-yl)phenyl)-1-(furan-3-yl) methanimine (1n). Light yellow solid; yield 60%. Mp 170–172 °C. ^{1}H NMR (400 MHz, chloroform-*d*) δ 8.44 (s, 1H, –CH=N–), 8.12 (d, J = 8.3 Hz, 2H, ArH), 8.07 (d, J = 8.1 Hz, 1H, ArH), 7.92–7.90 (m, 2H, ArH), 7.54–7.46 (m, 2H, ArH), 7.40–7.37 (m, 1H, ArH), 7.27 (d, J = 8.3 Hz, 2H, ArH), 6.97 (s, 1H, ArH). ^{13}C NMR (100 MHz, chloroform-*d*) δ 166.6, 153.5, 153.2, 151.7, 146.2, 143.5, 134.0, 130.1, 127.5 (2C), 125.3, 124.9, 124.1, 122.0, 120.6, 120.4 (2C), 106.8. HRMS (ESI) *m*/*z*: calculated for $C_{18}H_{13}N_2OS$ $[M + H]^+$: 305.0743, found: 305.0755.

(*E*)-*N*-(4-(Benzo[*d*]thiazol-2-yl)phenyl)-1-(thiophen-3-yl) methanimine (1o). Light yellow solid; yield 58%. Mp 162–164 °C. ^{1}H NMR (400 MHz, chloroform-*d*) δ 8.51 (s, 1H, –CH=N–), 8.12 (d, J = 8.2 Hz, 2H, ArH), 8.07 (d, J = 8.1 Hz, 1H, ArH), 7.90 (d, J = 7.9 Hz, 1H, ArH), 7.85 (s, 1H, ArH), 7.71 (d, J = 5.0 Hz, 1H, ArH), 7.51–7.47 (m, 1H, ArH), 7.41–7.36 (m, 2H, ArH), 7.29 (d, J = 8.2 Hz, 2H, ArH). ^{13}C NMR (100 MHz, chloroform-*d*) δ 167.6, 155.0, 154.5, 154.3, 140.6, 135.1, 131.2, 130.9, 128.6 (2C), 126.9, 126.3, 126.0, 125.1, 123.1, 121.6, 121.5 (2C). HRMS (ESI) *m*/*z*: calculated for $C_{18}H_{13}N_2S_2$ $[M + H]^+$: 321.0515, found: 321.0513.

(*E*)-*N*-(4-(Benzo[*d*]thiazol-2-yl)phenyl)-1-(1*H*-pyrrol-3-yl) methanimine (1p). White solid; yield 55%. Mp > 220 °C. ^{1}H NMR (400 MHz, DMSO-d_6) δ 11.41 (s, 1H, pyrrole), 8.48 (s, 1H, –CH=N–), 8.13 (d, J = 8.0 Hz, 1H, ArH), 8.08 (d, J = 8.1 Hz, 2H, ArH), 8.04 (d, J = 8.1 Hz, 1H, ArH), 7.56–7.52 (m, 1H, ArH), 7.47–7.43 (m, 2H, ArH), 7.30 (d, J = 8.1 Hz, 2H, ArH), 6.91 (s, 1H, ArH), 6.59 (s, 1H, ArH). ^{13}C NMR (100 MHz, DMSO-d_6) δ 167.1, 156.4, 155.6, 153.6, 134.3, 129.0, 128.2 (2C), 126.6, 125.3, 125.3, 123.0, 122.6, 122.2, 121.7 (2C), 120.5, 106.2. HRMS (ESI) *m*/*z*: calculated for $C_{18}H_{14}N_3S$ $[M + H]^+$: 304.0903, found: 304.0894.

(*E*)-*N*-(4-(Benzo[*d*]thiazol-2-yl)phenyl)-1-(thiophen-2-yl) methanimine (1q). Light green solid; yield 57%. Mp 184–185 °C. ^{1}H NMR (400 MHz, chloroform-*d*) δ 8.62 (s, 1H, –CH=N–), 8.12 (d, J = 8.1 Hz, 2H, ArH), 8.07 (d, J = 8.2 Hz, 1H, ArH), 7.90 (d, J = 8.0 Hz, 1H, ArH), 7.59–7.46 (m, 3H, ArH), 7.41–7.35 (m, 1H, ArH), 7.32 (d, J = 8.2 Hz, 2H, ArH), 7.18–7.14 (m, 1H, ArH). ^{13}C NMR (100 MHz, chloroform-*d*) δ 167.6, 154.2, 153.7, 153.7, 142.6, 135.0, 133.0, 131.3, 131.1, 128.6 (2C), 127.9, 126.4, 125.1, 123.1, 121.7 (2C), 121.6. HRMS (ESI) *m*/*z*: calculated for $C_{18}H_{12}N_2NaS_2$ $[M + Na]^+$: 343.0334, found: 343.0333.

(*E*)-*N*-(4-(Benzo[*d*]thiazol-2-yl)phenyl)-1-(5-nitrothiophen-3-yl)methanimine (1r). Yellow solid; yield 74%. Mp 213–215 °C. ^{1}H NMR (400 MHz, DMSO-d_6) δ 8.70 (s, 1H, –CH=N–), 8.60 (s, 1H, ArH), 8.42 (s, 1H, ArH), 8.16–8.14 (m, 3H, ArH), 8.06 (d, J = 8.2 Hz, 1H, ArH), 7.57–7.53 (m, 1H, ArH), 7.48–7.43 (m, 3H, ArH). ^{13}C NMR (100 MHz, DMSO-d_6) δ 166.7, 155.4, 153.6, 153.1, 152.1, 138.7, 138.1, 134.4, 130.8, 128.3 (2C), 127.2, 126.7, 125.5, 122.8, 122.3, 122.1 (2C). HRMS (ESI) *m*/*z*: calculated for $C_{18}H_{12}N_3O_2S_2$ $[M + H]^+$: 366.0365, found: 366.0360.

(*E*)-*N*-(4-(Benzo[*d*]thiazol-2-yl)phenyl)-1-(thiazol-4-yl) methanimine (1s). Golden solid; yield 69%. Mp 173–174 °C. ^{1}H NMR (400 MHz, chloroform-*d*) δ 8.93 (s, 1H, ArH), 8.72 (s, 1H, –CH=N–), 8.17–8.10 (m, 3H, ArH), 8.07 (d, J = 8.2 Hz, 1H, ArH), 7.91 (d, J = 8.0 Hz, 1H, ArH), 7.53–7.47 (m, 1H, ArH), 7.42–7.36 (m, 3H, ArH). ^{13}C NMR (100 MHz, chloroform-*d*) δ 167.5, 154.5, 154.2, 154.1, 153.7, 153.6, 135.1, 131.7, 128.6 (2C), 126.4, 125.2, 123.2, 122.3, 121.7 (2C), 121.6. HRMS (ESI) *m*/*z*: calculated for $C_{17}H_{11}N_3NaS_2$ $[M + Na]^+$: 344.0287, found: 344.0275.

(*E*)-*N*-(4-(Benzo[*d*]thiazol-2-yl)phenyl)-1-(thiazol-5-yl) methanimine (1t). Yellow solid; yield 72%. Mp 180–182 °C. ^{1}H

 This journal is © The Royal Society of Chemistry 2020

Open Access Article. Published on 07 2020. Downloaded on 2025/12/13 4:57:53.
This article is licensed under a Creative Commons Attribution-NonCommercial 3.0 Unported Licence.

NMR (400 MHz, chloroform-*d*) δ 8.95 (s, 1H, ArH), 8.71 (s, 1H, –CH=N–), 8.29 (s, 1H, ArH), 8.13 (d, J = 8.2 Hz, 2H, ArH), 8.07 (d, J = 8.2 Hz, 1H, ArH), 7.91 (d, J = 8.0 Hz, 1H, ArH), 7.53–7.47 (m, 1H, ArH), 7.41–7.37 (m, 1H, ArH), 7.32 (d, J = 8.2 Hz, 2H, ArH). ^{13}C NMR (100 MHz, chloroform-*d*) δ 167.3, 157.0, 154.2, 153.0, 151.3, 147.8, 138.3, 135.0, 131.9, 128.6 (2C), 126.4, 125.2, 123.2, 121.7, 121.6 (3C). HRMS (ESI) *m*/*z*: calculated for $C_{17}H_{12}N_3S_2$ $[M + H]^+$: 322.0467, found: 322.0471.

(*E*)-*N*-(4-(Benzo[*d*]thiazol-2-yl)phenyl)-1-(thiazol-2-yl) methanimine (1u). Light green solid; yield 64%. Mp 193–195 °C. ^{1}H NMR (400 MHz, chloroform-*d*) δ 8.75 (s, 1H, –CH=N–), 8.15 (d, J = 8.1 Hz, 2H, ArH), 8.08 (d, J = 8.2 Hz, 1H, ArH), 8.03 (d, J = 3.1 Hz, 1H, ArH), 7.91 (d, J = 8.0 Hz, 1H, ArH), 7.55 (d, J = 3.0 Hz, 1H, ArH), 7.53–7.47 (m, 1H, ArH), 7.42–7.36 (m, 3H, ArH). ^{13}C NMR (100 MHz, chloroform-*d*) δ 167.2, 166.9, 154.2, 153.8, 152.1, 144.8, 135.1, 132.5, 128.7 (2C), 126.4, 125.3, 123.2, 123.0, 121.9 (2C), 121.7. HRMS (ESI) *m*/*z*: calculated for $C_{17}H_{11}N_3NaS_2$ $[M + Na]^+$: 344.0287, found: 344.0271.

(*E*)-*N*-(4-(Thiazolo[4,5-*b*]pyridin-2-yl)phenyl)-1-(thiophen-3-yl)methanimine (4a). Light yellow solid; yield 32%. Mp 176–178 °C. ^{1}H NMR (400 MHz, DMSO-d_6) δ 8.72–8.68 (m, 2H, ArH and –CH=N–), 8.65 (d, J = 8.0 Hz, 1H, ArH), 8.27 (s, 1H, ArH), 8.20 (d, J = 8.1 Hz, 2H, ArH), 7.73–7.69 (m, 2H, ArH), 7.50–7.45 (m, 4.7 Hz, 1H, ArH), 7.42 (d, J = 8.1 Hz, 2H, ArH). ^{13}C NMR (100 MHz, DMSO-d_6) δ 170.1, 164.2, 156.5, 154.9, 148.4, 140.3, 133.1, 131.8, 129.7, 128.4 (2C), 128.3, 128.0, 125.4, 122.0 (2C), 120.3. HRMS (ESI) *m*/*z*: calculated for $C_{17}H_{11}N_3NaS_2$ $[M + Na]^+$: 344.0287, found: 344.0289.

(*E*)-*N*-(4-(4,5,6,7-Tetrahydrobenzo[*d*]thiazol-2-yl)phenyl)-1-(thiophen-3-yl) methanimine (4b). Khaki solid; yield 60%. Mp 150–151 °C. ^{1}H NMR (400 MHz, chloroform-*d*) δ 8.49 (s, 1H, –CH=N–), 7.91 (d, J = 8.2 Hz, 2H, ArH), 7.82 (s, 1H, ArH), 7.69 (d, J = 5.1 Hz, 1H, ArH), 7.41–7.37 (m, 1H, ArH), 7.22 (d, J = 8.2 Hz, 2H, ArH), 2.87–2.79 (m, 4H, CH_2), 1.94–1.86 (m, 4H, CH_2). ^{13}C NMR (100 MHz, chloroform-*d*) δ 163.1, 153.5, 151.9, 150.4, 139.7, 130.8, 129.6, 128.0, 126.1 (2C), 125.8, 124.9, 120.3 (2C), 25.9, 22.7, 22.4, 22.0. HRMS (ESI) *m*/*z*: calculated for $C_{18}H_{17}N_2S_2^+$ $[M + H]^+$: 325.0828, found: 325.0814.

(*E*)-*N*-(4-(Benzo[*d*]imidazo[2,1-*b*]thiazol-2-yl)phenyl)-1-(thiophen-3-yl) methanimine (4c). Khaki solid; yield 38%. Mp 162–163 °C. ^{1}H NMR (400 MHz, chloroform-*d*) δ 8.54 (s, 1H, –CH=N–), 7.98 (s, 1H, ArH), 7.90 (d, J = 8.1 Hz, 2H, ArH), 7.81 (s, 1H, ArH), 7.73–7.68 (m, 2H, ArH), 7.62 (d, J = 8.1 Hz, 1H, ArH), 7.49–7.43 (m, 1H, ArH), 7.40–7.32 (m, 2H, ArH), 7.28 (d, J = 8.1 Hz, 2H, ArH). ^{13}C NMR (100 MHz, chloroform-*d*) δ 153.0, 150.1, 147.1, 146.4, 139.9, 131.1, 130.6, 129.3, 129.2, 125.7, 125.2, 125.0 (2C), 124.9, 123.8, 123.4, 120.3 (2C), 111.6, 105.6. HRMS (ESI) *m*/*z*: calculated for $C_{20}H_{14}N_3S_2$ $[M + H]^+$: 360.0624, found: 360.0609.

(*E*)-*N*-(4-(Imidazo[1,2-*a*]pyridin-2-yl)phenyl)-1-(thiophen-3-yl)methanimine (4d). Light yellow solid; yield 34%. Mp 203–205 °C. ^{1}H NMR (400 MHz, chloroform-*d*) δ 8.53 (s, 1H, –CH=N–), 8.10 (d, J = 6.8 Hz, 1H, ArH), 7.98 (d, J = 8.5 Hz, 2H, ArH), 7.85 (s, 1H, ArH), 7.80 (s, 1H, ArH), 7.70 (d, J = 5.1 Hz, 1H, ArH), 7.62 (d, J = 9.1 Hz, 1H, ArH), 7.40–7.36 (m, 1H, ArH), 7.28 (d, J = 8.3 Hz, 2H, ArH), 7.19–7.13 (m, 1H, ArH), 6.79–6.74 (m, 1H, ArH). ^{13}C NMR (100 MHz, chloroform-*d*) δ 153.1, 150.6, 144.7, 144.5, 139.8, 130.5, 129.2, 125.8 (2C), 125.7, 124.9, 124.5, 123.6, 120.3 (2C), 116.5, 111.4, 106.9. HRMS (ESI) *m*/*z*: calculated for $C_{18}H_{14}N_3S$ $[M + H]^+$: 304.0903, found: 304.0897.

(*E*)-*N*-(4-(7-Fluorobenzo[*d*]thiazol-2-yl)phenyl)-1-(thiophen-3-yl)methanimine (4e). Light yellow solid; yield 38%. Mp 166–167 °C. ^{1}H NMR (400 MHz, chloroform-*d*) δ 8.50 (s, 1H, –CH=N–), 8.12 (d, J = 8.5 Hz, 2H, ArH), 7.88–7.85 (m, 2H, ArH), 7.71 (d, J = 5.1 Hz, 1H, ArH), 7.48–7.40 (m, 2H, ArH), 7.30 (d, J = 8.5 Hz, 2H, ArH), 7.13–7.09 (m, 1H, ArH). ^{13}C NMR (100 MHz, chloroform-*d*) δ 167.6 (d, J = 1.7 Hz), 156.1 (d, J = 250.1 Hz), 156.0 (d, J = 2.5 Hz), 154.2, 153.8, 139.5, 130.2, 129.5, 127.7 (2C), 126.2 (d, J = 7.3 Hz), 125.9, 124.9, 121.1 (d, J = 16.5 Hz), 120.5 (2C), 117.9 (d, J = 3.5 Hz), 109.5 (d, J = 18.7 Hz). HRMS (ESI) *m*/*z*: calculated for $C_{18}H_{12}FN_2S_2$ $[M + H]^+$: 339.0420, found: 339.0418.

(*E*)-*N*-(4-(6-Fluorobenzo[*d*]thiazol-2-yl)phenyl)-1-(thiophen-3-yl)methanimine (4f). Light yellow solid; yield 52%. Mp 187–189 °C. ^{1}H NMR (400 MHz, chloroform-*d*) δ 8.50 (s, 1H, –CH=N–), 8.08 (d, J = 8.3 Hz, 2H, ArH), 8.00 (dd, J = 8.8, 4.8 Hz, 1H, ArH), 7.86 (s, 1H, ArH), 7.70 (d, J = 4.9 Hz, 1H, ArH), 7.60–7.56 (m, 1H, ArH), 7.43–7.39 (m, 1H, ArH), 7.29 (d, J = 8.3 Hz, 2H, ArH), 7.25–7.19 (m, 1H, ArH). ^{13}C NMR (100 MHz, chloroform-*d*) δ 166.3 (d, J = 3.3 Hz), 159.4 (d, J = 245.7 Hz), 154.1, 153.5, 149.8 (d, J = 1.8 Hz), 139.5, 135.0 (d, J = 11.1 Hz), 130.1, 129.8, 127.4 (2C), 125.9, 124.9, 122.9 (d, J = 9.2 Hz), 120.5 (2C), 113.9 (d, J = 24.6 Hz), 106.8 (d, J = 26.8 Hz). HRMS (ESI) *m*/*z*: calculated for $C_{18}H_{12}FN_2S_2$ $[M + H]^+$: 339.0420, found: 339.0431.

(*E*)-*N*-(4-(5-Fluorobenzo[*d*]thiazol-2-yl)phenyl)-1-(thiophen-3-yl)methanimine (4g). Khaki solid; yield 51%. Mp 183–185 °C. ^{1}H NMR (400 MHz, chloroform-*d*) δ 8.49 (s, 1H, –CH=N–), 8.09 (d, J = 8.5 Hz, 2H, ArH), 7.85 (dd, J = 3.0, 1.2 Hz, 1H, ArH), 7.81 (dd, J = 8.8, 5.1 Hz, 1H, ArH), 7.73 (dd, J = 9.6, 2.5 Hz, 1H, ArH), 7.70 (d, J = 5.1 Hz, 1H, ArH), 7.40 (dd, J = 5.1, 2.9 Hz, 1H, ArH), 7.28 (d, J = 8.5 Hz, 2H, ArH), 7.17–7.13 (m, 1H, ArH). ^{13}C NMR (100 MHz, chloroform-*d*) δ 169.0, 160.9 (d, J = 243.2 Hz), 154.1, 154.1 (d, J = 12.1 Hz), 153.6, 139.5, 130.1, 129.8, 129.3 (d, J = 1.9 Hz), 127.5 (2C), 125.9, 124.9, 121.2 (d, J = 9.9 Hz), 120.5 (2C), 112.7 (d, J = 25.0 Hz), 108.2 (d, J = 23.6 Hz). HRMS (ESI) *m*/*z*: calculated for $C_{18}H_{12}FN_2S_2$ $[M + H]^+$: 339.0420, found: 339.0423.

(*E*)-*N*-(4-(4-Fluorobenzo[*d*]thiazol-2-yl)phenyl)-1-(thiophen-3-yl)methanimine (4h). Yellow solid; yield 36%. Mp 153–154 °C. ^{1}H NMR (400 MHz, chloroform-*d*) δ 8.50 (s, 1H, –CH=N–), 8.15 (d, J = 8.6 Hz, 2H, ArH), 7.86 (dd, J = 2.9, 1.1 Hz, 1H, ArH), 7.70 (dd, J = 5.1, 0.9 Hz, 1H, ArH), 7.66 (dd, J = 8.0, 0.8 Hz, 1H, ArH), 7.41 (dd, J = 5.0, 2.6 Hz, 1H, ArH), 7.36–7.29 (m, 1H, ArH), 7.28 (d, J = 8.6 Hz, 2H, ArH), 7.19 (ddd, J = 10.4, 8.1, 0.8 Hz, 1H, ArH). ^{13}C NMR (100 MHz, chloroform-*d*) δ 167.1, 154.8 (d, J = 257.2 Hz), 154.2, 153.7, 142.0 (d, J = 13.4 Hz), 139.5, 136.6 (d, J = 3.6 Hz), 130.1, 129.6, 127.8 (2C), 125.9, 124.9, 124.7 (d, J = 7.1 Hz), 120.5 (2C), 116.3 (d, J = 4.3 Hz), 111.0 (d, J = 18.0 Hz). HRMS (ESI) *m*/*z*: calculated for $C_{18}H_{12}FN_2S_2$ $[M + H]^+$: 339.0420, found: 339.0417.

(*E*)-*N*-(4-(6-Ethoxybenzo[*d*]thiazol-2-yl)phenyl)-1-(thiophen-3-yl)methanimine (4i). Yellow solid; yield 32%. Mp 181–183 °C. ^{1}H NMR (400 MHz, chloroform-*d*) δ 8.51 (s, 1H, –CH=N–), 8.06 (d, J = 8.2 Hz, 2H, ArH), 7.93 (d, J = 8.9 Hz, 1H, ArH), 7.85 (s, 1H, ArH), 7.70 (d, J = 4.8 Hz, 1H, ArH), 7.41 (s, 1H, ArH), 7.34 (s, 1H, ArH), 7.29 (d, J = 8.2 Hz, 2H, ArH), 7.08 (d, J = 9.4 Hz, 1H, ArH),

Open Access Article. Published on 07 2020. Downloaded on 2025/12/13 4:57:53.
This article is licensed under a Creative Commons Attribution-NonCommercial 3.0 Unported Licence.

4.11 (q, J = 6.9 Hz, 2H, CH_2), 1.47 (t, J = 6.9 Hz, 3H, CH_3). ^{13}C NMR (100 MHz, chloroform-*d*) δ 164.0, 156.0, 153.9, 152.9, 147.7, 139.6, 135.3, 130.3, 129.9, 127.2 (2C), 125.9, 124.9, 122.5, 120.4 (2C), 115.0, 103.9, 63.1, 13.8. HRMS (ESI) *m*/*z*: calculated for $C_{20}H_{16}N_2NaOS_2$ $[M + Na]^+$: 387.0596, found: 387.0613.

(*E*)-*N*-(4-(6-Methylbenzo[*d*]thiazol-2-yl)phenyl)-1-(thiophen-3-yl)methanimine (4j). Golden solid; yield 37%. Mp 191–192 °C. ^{1}H NMR (400 MHz, chloroform-*d*) δ 8.50 (s, 1H, –CH=N–), 8.10 (d, J = 8.3 Hz, 2H, ArH), 7.94 (d, J = 8.3 Hz, 1H, ArH), 7.85 (s, 1H, ArH), 7.72–7.68 (m, 2H, ArH), 7.43–7.38 (m, 1H, ArH), 7.32–7.27 (m, 3H, ArH), 2.50 (s, 3H, CH_3). ^{13}C NMR (100 MHz, chloroform-*d*) δ 166.6, 155.0, 154.2, 152.3, 140.6, 135.3, 135.2, 131.3, 131.0, 128.4 (2C), 127.9, 126.9, 125.9, 122.6, 121.5 (2C), 121.4, 21.6. HRMS (ESI) *m*/*z*: calculated for $C_{19}H_{15}N_2S_2$ $[M + H]^+$: 335.0671, found: 335.0678.

(*E*)-*N*-Methyl-2-(4-((thiophen-3-ylmethylene)amino)phenyl) benzo[*d*]thiazol-6-amine (4k). Yellow solid; yield 59%. Mp 200–201 °C. ^{1}H NMR (400 MHz, DMSO-d_6) δ 8.67 (s, 1H, –CH=N–), 8.23 (s, 1H, ArH), 7.99 (d, J = 8.2 Hz, 2H, ArH), 7.72 (d, J = 8.8 Hz, 1H, ArH), 7.70–7.68 (m, 1H, ArH), 7.65–7.64 (m, 1H, ArH), 7.35 (d, J = 8.2 Hz, 2H, ArH), 7.04 (s, 1H, ArH), 6.81 (d, J = 8.8 Hz, 1H, ArH), 6.11 (q, J = 5.0 Hz, 1H, NH), 2.75 (d, J = 4.9 Hz, 3H, CH_3). ^{13}C NMR (100 MHz, DMSO-d_6) δ 160.0, 155.7, 152.9, 148.4, 145.0, 140.4, 136.7, 132.6, 131.0, 127.8, 127.4 (2C), 125.4, 122.9, 121.8 (2C), 114.3, 100.3, 29.9. HRMS (ESI) *m*/*z*: calculated for $C_{19}H_{16}N_3S_2$ $[M + H]^+$: 350.0780, found: 350.0757.

(*E*)-*N*,*N*-Dimethyl-2-(4-((thiophen-3-ylmethylene)amino) phenyl)benzo[*d*]thiazol-6-amine (4l). Orange solid; yield 60%. Mp 177–178 °C. ^{1}H NMR (400 MHz, DMSO-d_6) δ 8.68 (s, 1H, –CH=N–), 8.24 (s, 1H, ArH), 8.02 (d, J = 8.6 Hz, 2H, ArH), 7.83 (d, J = 9.1 Hz, 1H, ArH), 7.71–7.69 (m, 1H, ArH), 7.65–7.64 (m, 1H, ArH), 7.36 (d, J = 8.5 Hz, 2H, ArH), 7.32 (s, 1H, ArH), 7.01 (d, J = 9.0 Hz, 1H, ArH), 3.00 (s, 6H, CH_3). ^{13}C NMR (100 MHz, DMSO-d_6) δ 161.1, 155.8, 153.1, 148.7, 145.3, 140.4, 136.6, 132.7, 130.8, 127.9, 127.5 (2C), 125.4, 122.8, 1218 (2C), 113.3, 103.1, 40.5. HRMS (ESI) *m*/*z*: calculated for $C_{20}H_{18}N_3S_2^+[M + H]^+$: 364.0937, found: 364.0948.

(*E*)-2-(4-((Thiophen-3-ylmethylene)amino)phenyl)benzo[*d*] thiazole-6-carboxylic acid (4m). Yellow solid; yield 86%. Mp: >220 °C. ^{1}H NMR (400 MHz, DMSO-d_6) δ 13.16 (br, 1H, COOH), 8.77 (s, 1H, –CH=N–), 8.68 (s, 1H, ArH), 8.26 (s, 1H, ArH), 8.15 (d, J = 8.1 Hz, 2H, ArH), 8.12–8.06 (m, 2H, ArH), 7.71–7.69 (m, 1H, ArH), 7.66–7.64 (m, 1H, ArH), 7.40 (d, J = 8.1 Hz, 2H, ArH). ^{13}C NMR (100 MHz, DMSO-d_6) δ 170.4, 166.9, 156.4, 156.4, 154.6, 140.3, 134.5, 133.1, 129.8, 128.6 (2C), 127.9, 127.5, 127.5, 125.4, 124.3, 122.4, 121.9 (2C). HRMS (ESI) *m*/*z*: calculated for $C_{19}H_{13}N_2O_2S_2$ $[M + H]^+$: 365.0413, found: 365.0428.

(*E*)-*N*-Methyl-2-(4-((thiophen-3-ylmethylene)amino)phenyl) benzo[*d*]thiazole-6- carboxamide (4n). Yellow solid; yield 72%. Mp: >220 °C. ^{1}H NMR (400 MHz, DMSO-d_6) δ 8.69 (s, 1H, –CH=N–), 8.61–8.55 (m, 2H, ArH and –(C=O)NH–), 8.26 (s, 1H, ArH), 8.15 (d, J = 8.5 Hz, 2H, ArH), 8.09 (d, J = 8.5 Hz, 1H, ArH), 7.98 (d, J = 8.5 Hz, 1H, ArH), 7.72–7.68 (m, 1H, ArH), 7.66–7.65 (m, 1H, ArH), 7.40 (d, J = 8.5 Hz, 2H, ArH), 2.84 (d, J = 4.4 Hz, 3H, CH_3). ^{13}C NMR (100 MHz, DMSO-d_6) δ 169.2, 166.0, 156.4, 155.2, 154.5, 140.3, 134.4, 133.0, 131.5, 129.9, 128.5 (2C), 127.9, 125.6, 125.4, 122.2, 121.9 (2C), 121.6, 26.4. HRMS (ESI) *m*/*z*: calculated for $C_{20}H_{15}N_3NaOS_2$ $[M + Na]^+$: 400.0549, found: 400.0565.

(*E*)-*N*-(4-(Benzo[*d*]thiazol-2-yloxy)phenyl)-1-(thiophen-3-yl) methanimine (4o). White solid; yield 18%. Mp 95–97 °C. ^{1}H NMR (400 MHz, DMSO-d_6) δ 8.66 (s, 1H, –CH=N–), 8.21 (s, 1H, ArH), 7.94 (d, J = 8.0 Hz, 1H, ArH), 7.73–7.67 (m, 2H, ArH), 7.66–7.61 (m, 1H, ArH), 7.49 (d, J = 8.4 Hz, 2H, ArH), 7.46–7.41 (m, 1H, ArH), 7.38–7.30 (m, 3H, ArH). ^{13}C NMR (100 MHz, DMSO-d_6) δ 171.9, 155.8, 152.1, 149.9, 148.6, 140.4, 132.4, 131.8, 127.8, 126.5, 125.4, 124.2, 122.4 (2C), 122.2, 121.7 (2C), 121.1. HRMS (ESI) *m*/*z*: calculated for $C_{18}H_{13}N_2OS_2$ $[M + H]^+$: 337.0464, found: 337.0474.

(*E*)-*N*-(4-(Benzo[*d*]thiazol-2-ylthio)phenyl)-1-(thiophen-3-yl) methanimine (4p). White solid; yield 20%. Mp 109–111 °C. ^{1}H NMR (400 MHz, DMSO-d_6) δ 8.66 (s, 1H, –CH=N–), 8.27 (s, 1H, ArH), 7.94 (d, J = 8.0 Hz, 1H, ArH), 7.87–7.80 (m, 3H, ArH), 7.72–7.68 (m, 1H, ArH), 7.67–7.63 (m, 1H, ArH), 7.48–7.43 (m, 1H, ArH), 7.41–7.31 (m, 3H, ArH). ^{13}C NMR (100 MHz, DMSO-d_6) δ 169.7, 156.8, 154.0, 153.5, 140.2, 136.6 (2C), 134.8, 133.1, 127.9, 126.4, 125.4, 125.1, 124.4, 122.7 (2C), 121.7, 121.3. HRMS (ESI) *m*/*z*: calculated for $C_{18}H_{13}N_2S_3$ $[M + H]^+$: 353.0235, found: 353.0232.

Synthesis of (*E*)-2-((benzo[*d*]thiazol-2-ylimino)methyl)-6-methoxyphenol (1e)

The catalytic amount of acetic acid was added to a solution of 3e (0.5 mmol) and 2-hydroxy-3-methoxybenzaldehyde (0.6 mmol) in MeOH (4 mL), the mixture was stirred at reflux for 2 h. The resulting precipitate was isolated by suction filtration and washed with MeOH to give the pure product **1e**. Orange solid; yield 32%. Mp 170–172 °C. ^{1}H NMR (400 MHz, chloroform-*d*) δ 12.44 (s, 1H, OH), 9.26 (s, 1H, –CH=N–), 7.96 (d, J = 8.2 Hz, 1H, ArH), 7.83 (d, J = 8.0 Hz, 1H, ArH), 7.51–7.45 (m, 1H, ArH), 7.39–7.33 (m, 1H, ArH), 7.13 (d, J = 7.9 Hz, 1H, ArH), 7.06 (d, J = 8.0 Hz, 1H, ArH), 6.95–6.89 (m, 1H, ArH), 3.93 (s, 3H, $-CH_3$). ^{13}C NMR (100 MHz, chloroform-*d*) δ 167.9, 166.4, 151.1, 150.5, 147.5, 133.7, 125.7, 124.3, 124.2, 122.0, 120.7, 118.3, 117.4, 115.8, 55.3. HRMS (ESI) *m*/*z*: calculated for $C_{15}H_{12}N_2NaO_2S$ $[M + Na]^+$: 307.0512, found: 307.0509.

Synthesis of 2-(((4-(benzo[*d*]thiazol-2-yl)phenyl)amino) methyl)-6-methoxy-phenol (1f)

$NaBH_4$ (0.84 mmol) was added to a suspension of **1a** (0.42 mmol) in MeOH (6 mL) and stirred at room temperature for 1 h. Upon completion, MeOH was removed under reduced pressure. The crude mixture was then purified by flash column chromatography in a mixture of petroleum ether and ethyl acetate to yield the pure product **1f**. Light yellow solid; yield 66%. Mp 187–188 °C. ^{1}H NMR (400 MHz, DMSO-d_6) δ 8.79 (s, 1H, OH), 8.00 (d, J = 7.4 Hz, 1H, ArH), 7.89 (d, J = 8.1 Hz, 1H, ArH), 7.78 (d, J = 8.4 Hz, 2H, ArH), 7.46–7.43 (m, 1H, ArH), 7.35–7.31 (m, 1H, ArH), 6.88–6.84 (m, 2H, ArH and NH), 6.82–6.80 (m, 1H, ArH), 6.73–6.68 (m, 3H, ArH), 4.30 (d, J = 5.9 Hz, 2H, CH_2), 3.80 (s, 3H, CH_3). ^{13}C NMR (100 MHz, DMSO-d_6) δ 168.0, 153.9, 151.6, 147.3, 143.8, 133.7, 128.6, 126.2, 125.5, 124.3, 121.8, 121.7, 120.0,

 This journal is © The Royal Society of Chemistry 2020

Open Access Article. Published on 07 2020. Downloaded on 2025/12/13 4:57:53.
This article is licensed under a Creative Commons Attribution-NonCommercial 3.0 Unported Licence.

120.0, 118.6, 111.9, 110.4, 55.8, 40.8. HRMS (ESI) *m*/*z*: calculated for $C_{21}H_{19}N_2O_2S$ $[M + H]^+$: 363.1162, found: 363.1190.

Synthesis of *N*-(4-(benzo[*d*]thiazol-2-yl)phenyl)-2-hydroxy-3-methoxybenzamide (1g)

2-Hydroxy-3-methoxybenzoyl chloride (0.53 mmol) was dissolved in Et_2O (0.5 mL) and then added dropwise to a stirring solution of **3a** (0.44 mmol) and $NaHCO_3$ (0.88 mmol) in Et_2O (1 mL) and H_2O (0.5 mL) at 0 °C. Then the reaction was allowed to warm to room temperature and stirred for 12 h. The resulting precipitate was isolated by suction filtration and washed with H_2O (2 mL), 2 N HCl (2 mL) and H_2O (2 mL) sequentially to yield the pure product **1g**. White solid; yield 14%. Mp 215–216 °C. ^{1}H NMR (400 MHz, DMSO-d_6) δ 11.33 (s, 1H, OH), 10.60 (s, 1H, –(C=O)NH–), 8.13–8.09 (m, 3H, ArH), 8.04 (d, J = 8.2 Hz, 1H, ArH), 7.93 (d, J = 8.4 Hz, 2H, ArH), 7.53 (d, J = 7.8 Hz, 2H, ArH), 7.47–7.42 (m, 1H, ArH), 7.18 (d, J = 8.0 Hz, 1H, ArH), 6.96–6.90 (m, 1H, ArH), 3.84 (s, 3H, CH_3). ^{13}C NMR (100 MHz, DMSO-d_6) δ 167.0, 166.8, 153.6, 148.4, 148.3, 141.1, 134.3, 128.4, 127.9 (2C), 126.6, 125.3, 122.6, 122.2, 120.9 (2C), 120.1, 118.6, 118.0, 115.5, 56.0. HRMS (ESI) *m*/*z*: calculated for $C_{21}H_{16}N_2NaO_3S$ $[M + Na]^+$: 399.0774, found: 399.0774.

Plasmid and pseudovirus production

To produce MERS spike protein pseudotyped HIV virions, we constructed a MERS spike protein (MERS-S) expression plasmid. The codon-optimized gene of full-length S protein of MERS-CoV (Genebank: AFS88936), with replacement of the N-terminal signal peptide (aa 1–17) with CD5 signal sequence, were synthesized (Inovogen, China) and insertion into pcDNA3.1 vector, verified by sequencing. A HIV backbone vector pNL4-3. Luc.R-E- was used for pseudovirus package. 293T cells were co-transfected with MERS spike protein expression plasmid plus pNL4.3LucR-E- plasmid using X-tremeGENE DNA HP Transfection Reagent (Roche) according the manufacturer's instructions.[29] At 72 h post-transfection, supernatants were harvested and filtered through 0.45 μm filter, the filtered supernatant was further concentrated 10 folds by ultracentrifugation with 100 kDa cut-off, aliquoted and stored at −80 °C as stock vial. The p24 level of pseudovirus stock solution was determined by ELISA kit according to the manual (ab218268, Abcam).

Compound library and HTS screening

Compound library samples were orthogonally pooled as mixtures of 10 compounds per well at 2 μg mL^{-1} each, with duplicate representation for each compound. This bidirectional orthogonal pooling strategy allows for greater screening efficiency and throughput for large compound libraries. The pooling of compound library was prepared as described previously.[52]

Test compounds were freshly prepared from initial dimethyl sulfoxide (DMSO) stocks, 80 cocktails per plate. Huh-7 cells were then trypsinized, counted and seeded at a final concentration of 104 cells per well. Plates were placed overnight in a CO_2 incubator. The following day, samples were then added with an automatic liquid handler (FX from Beckman–Coulter). Finally, the pseudotyped virus, thawed and diluted immediately prior to use in cell culture medium, was added under a BSL-2 hood using Hydra (Thermo Fisher Scientific). The final concentration of DMSO in all wells was maintained at 2%. The plates were incubated at 37 °C in a humidified CO_2 incubator for 48 h. Bright-Glo substrate (Promega) was added directly to each well and cell lysis was allowed to proceed in the dark for 5 min.

Cytotoxic effect of compounds was assayed by MTT method which evaluated the reduction product of MTT by cellular succinate dehydrogenase as an indicator of cell liability. Toxicity was calculated as 100% minus percentage of $OD_{@570}$ readout each well against the control well with no drug, 100% − $OD_{@570}$ (compound)/$OD_{@570}$ (control) × 100%.

Luciferase activity was measured using the Envision microplate luminometer (PerkinElmer). Inhibition was calculated as 100% minus percentage of luciferase readout each well against the control well with no drug, 100% − Luc (compound)/Luc (control) × 100%.

Measurement of IC_{50} and CC_{50}

For determining CC_{50} and IC_{50}, compounds were serially diluted and assayed as described for the HTS screening, CC_{50} and IC_{50} were determined by regression analysis using 4 parameter regression.

Conflicts of interest

There are no conflicts of interest to declare.

Acknowledgements

This work was supported by the National Key Research and Development Program of China (2018YFC1200604). The pNL4.3.Luc.R-.E- and MERS-S expression plasmid was kindly gifted by Dr Shibo Jiang and Dr Lu Lu from Fudan University.

Notes and references

1 A. Zumla, D. S. Hui and S. Perlman, *Lancet*, 2015, **386**, 995–1007.
2 Y. M. Arabi, H. H. Balkhy, F. G. Hayden, A. Bouchama, T. Luke, J. K. Baillie, A. Al-Omari, A. H. Hajeer, M. Senga, M. R. Denison, J. S. Nguyen-Van-Tam, N. Shindo, A. Bermingham, J. D. Chappell, M. D. Van Kerkhove and R. A. Fowler, *N. Engl. J. Med.*, 2017, **376**, 584–594.
3 A. M. Zaki, S. van Boheemen, T. M. Bestebroer, A. D. Osterhaus and R. A. Fouchier, *N. Engl. J. Med.*, 2012, **367**, 1814–1820.
4 D. S. Hui, S. Perlman and A. Zumla, *Lancet Respir. Med.*, 2015, **3**, 509–510.
5 E. I. Azhar, S. A. El-Kafrawy, S. A. Farraj, A. M. Hassan, M. S. Al-Saeed, A. M. Hashem and T. A. Madani, *N. Engl. J. Med.*, 2014, **370**, 2499–2505.

Open Access Article. Published on 07 2020. Downloaded on 2025/12/13 4:57:53.
This article is licensed under a Creative Commons Attribution-NonCommercial 3.0 Unported Licence.

6 M. Cotten, S. J. Watson, P. Kellam, A. A. Al-Rabeeah, H. Q. Makhdoom, A. Assiri, J. A. Al-Tawfiq, R. F. Alhakeem, H. Madani, F. A. AlRabiah, S. A. Hajjar, W. N. Al-nassir, A. Albarrak, H. Flemban, H. H. Balkhy, S. Alsubaie, A. L. Palser, A. Gall, R. Bashford-Rogers, A. Rambaut, A. I. Zumla and Z. A. Memish, *Lancet*, 2013, **382**, 1993–2002.

7 R. Breban, J. Riou and A. Fontanet, *Lancet*, 2013, **382**, 694–699.

8 A. Assiri, J. A. Al-Tawfiq, A. A. Al-Rabeeah, F. A. Al-Rabiah, S. Al-Hajjar, A. Al-Barrak, H. Flemban, W. N. Al-Nassir, H. H. Balkhy, R. F. Al-Hakeem, H. Q. Makhdoom, A. I. Zumla and Z. A. Memish, *Lancet Infect. Dis.*, 2013, **13**, 752–761.

9 R. Alexpandi, J. F. De Mesquita, S. K. Pandian and A. V. Ravi, *Front. Microbiol.*, 2020, **11**, 1796.

10 W. R. Ferraz, R. A. Gomes, A. L. S. Novaes and G. H. G. Trossini, *Future Med. Chem.*, 2020, **12**, 1815–1828.

11 D. Gentile, V. Patamia, A. Scala, M. T. Sciortino, A. Piperno and A. Rescifina, *Mar. Drugs*, 2020, **18**, 225.

12 A. K. Ghosh, M. Brindisi, D. Shahabi, M. E. Chapman and A. D. Mesecar, *ChemMedChem*, 2020, **15**, 907–932.

13 M. Hagar, H. A. Ahmed, G. Aljohani and O. A. Alhaddad, *Int. J. Mol. Sci.*, 2020, **21**, 3922.

14 S. T. Ngo, N. Quynh Anh Pham, L. Thi Le, D. H. Pham and V. V. Vu, *J. Chem. Inf. Model.*, 2020, DOI: 10.1021/acs.jcim.0c00491.

15 O. O. Olubiyi, M. Olagunju, M. Keutmann, J. Loschwitz and B. Strodel, *Molecules*, 2020, **25**, 3193.

16 S. Shahinshavali, K. A. Hossain, A. Kumar, A. G. Reddy, D. Kolli, A. Nakhi, M. V. B. Rao and M. Pal, *Tetrahedron Lett.*, 2020, **61**, 152336.

17 L. Zhang, D. Lin, X. Sun, U. Curth, C. Drosten, L. Sauerhering, S. Becker, K. Rox and R. Hilgenfeld, *Science*, 2020, **368**, 409–412.

18 B. Cao, Y. Wang, D. Wen, W. Liu, J. L. Wang, G. Fan, L. Ruan, B. Song, Y. Cai, M. Wei, X. Li, J. Xia, N. Chen, J. Xiang, T. Yu, T. Bai, X. Xie, L. Zhang, C. Li, Y. Yuan, H. Chen, H. D. Li, H. Huang, S. Tu, F. Gong, Y. Liu, Y. Wei, C. Dong, F. Zhou, X. Gu, J. Xu, Z. Liu, Y. Zhang, H. Li, L. Shang, K. Wang, K. Li, X. Zhou, X. Dong, Z. Qu, S. Lu, X. Hu, S. Ruan, S. Luo, J. Wu, L. Peng, F. Cheng, L. Pan, J. Zou, C. Jia, J. Wang, X. Liu, S. Wang, X. Wu, Q. Ge, J. He, H. Zhan, F. Qiu, L. Guo, C. Huang, T. Jaki, F. G. Hayden, P. W. Horby, D. Zhang and C. Wang, *N. Engl. J. Med.*, 2020, **382**, 1787–1799.

19 M. Wang, R. Cao, L. Zhang, X. Yang, J. Liu, M. Xu, Z. Shi, Z. Hu, W. Zhong and G. Xiao, *Cell Res.*, 2020, **30**, 269–271.

20 D. Falzarano, E. de Wit, A. L. Rasmussen, F. Feldmann, A. Okumura, D. P. Scott, D. Brining, T. Bushmaker, C. Martellaro, L. Baseler, A. G. Benecke, M. G. Katze, V. J. Munster and H. Feldmann, *Nat. Med.*, 2013, **19**, 1313–1317.

21 V. Kumar, J. S. Shin, J. J. Shie, K. B. Ku, C. Kim, Y. Y. Go, K. F. Huang, M. Kim and P. H. Liang, *Antiviral Res.*, 2017, **141**, 101–106.

22 A. H. de Wilde, D. Jochmans, C. C. Posthuma, J. C. Zevenhoven-Dobbe, S. van Nieuwkoop, T. M. Bestebroer, B. G. van den Hoogen, J. Neyts and E. J. Snijder, *Antimicrob. Agents Chemother.*, 2014, **58**, 4875–4884.

23 T. P. Sheahan, A. C. Sims, R. L. Graham, V. D. Menachery, L. E. Gralinski, J. B. Case, S. R. Leist, K. Pyrc, J. Y. Feng, I. Trantcheva, R. Bannister, Y. Park, D. Babusis, M. O. Clarke, R. L. Mackman, J. E. Spahn, C. A. Palmiotti, D. Siegel, A. S. Ray, T. Cihlar, R. Jordan, M. R. Denison and R. S. Baric, *Sci. Transl. Med.*, 2017, **9**(396), eaal3653.

24 T. P. Sheahan, A. C. Sims, S. R. Leist, A. Schafer, J. Won, A. J. Brown, S. A. Montgomery, A. Hogg, D. Babusis, M. O. Clarke, J. E. Spahn, L. Bauer, S. Sellers, D. Porter, J. Y. Feng, T. Cihlar, R. Jordan, M. R. Denison and R. S. Baric, *Nat. Commun.*, 2020, **11**, 222.

25 M. H. Lin, D. C. Moses, C. H. Hsieh, S. C. Cheng, Y. H. Chen, C. Y. Sun and C. Y. Chou, *Antiviral Res.*, 2018, **150**, 155–163.

26 H. Lee, J. Ren, R. P. Pesavento, I. Ojeda, A. J. Rice, H. Lv, Y. Kwon and M. E. Johnson, *Bioorg. Med. Chem.*, 2019, **27**, 1981–1989.

27 L. Lu, S. Xia, T. Ying and S. Jiang, *Emerging Microbes Infect.*, 2015, **4**, e37.

28 J. Gao, G. Lu, J. Qi, Y. Li, Y. Wu, Y. Deng, H. Geng, H. Li, Q. Wang, H. Xiao, W. Tan, J. Yan and G. F. Gao, *J. Virol.*, 2013, **87**, 13134–13140.

29 L. Lu, Q. Liu, Y. Zhu, K. H. Chan, L. Qin, Y. Li, Q. Wang, J. F. Chan, L. Du, F. Yu, C. Ma, S. Ye, K. Y. Yuen, R. Zhang and S. Jiang, *Nat. Commun.*, 2014, **5**, 3067.

30 C. Wang, S. Xia, P. Zhang, T. Zhang, W. Wang, Y. Tian, G. Meng, S. Jiang and K. Liu, *J. Med. Chem.*, 2018, **61**, 2018–2026.

31 T. Ying, L. Du, T. W. Ju, P. Prabakaran, C. C. Lau, L. Lu, Q. Liu, L. Wang, Y. Feng, Y. Wang, B. J. Zheng, K. Y. Yuen, S. Jiang and D. S. Dimitrov, *J. Virol.*, 2014, **88**, 7796–7805.

32 Y. Li, Y. Wan, P. Liu, J. Zhao, G. Lu, J. Qi, Q. Wang, X. Lu, Y. Wu, W. Liu, B. Zhang, K. Y. Yuen, S. Perlman, G. F. Gao and J. Yan, *Cell Res.*, 2015, **25**, 1237–1249.

33 J. H. Beigel, J. Voell, P. Kumar, K. Raviprakash, H. Wu, J.-A. Jiao, E. Sullivan, T. Luke and R. T. Davey, *Lancet Infect. Dis.*, 2018, **18**, 410–418.

34 N. K. Alharbi, E. Padron-Regalado, C. P. Thompson, A. Kupke, D. Wells, M. A. Sloan, K. Grehan, N. Temperton, T. Lambe, G. Warimwe, S. Becker, A. V. S. Hill and S. C. Gilbert, *Vaccine*, 2017, **35**, 3780–3788.

35 B. L. Haagmans, J. M. A. van den Brand, V. S. Raj, A. Volz, P. Wohlsein, S. L. Smits, D. Schipper, T. M. Bestebroer, N. Okba, R. Fux, A. Bensaid, D. S. Foz, T. Kuiken, W. Baumgartner, J. Segales, G. Sutter and A. D. M. E. Osterhaus, *Science*, 2016, **351**, 77–81.

36 Y. Zhou, S. Jiang and L. Du, *Expert Rev. Vaccines*, 2018, **17**, 677–686.

37 S. Su, G. Wong, W. Shi, J. Liu, A. C. K. Lai, J. Zhou, W. Liu, Y. Bi and G. F. Gao, *Trends Microbiol.*, 2016, **24**, 490–502.

38 J. F. Chan, S. K. Lau and P. C. Woo, *J. Formosan Med. Assoc.*, 2013, **112**, 372–381.

39 S. van Boheemen, M. de Graaf, C. Lauber, T. M. Bestebroer, V. S. Raj, A. M. Zaki, A. D. Osterhaus, B. L. Haagmans,

 This journal is © The Royal Society of Chemistry 2020

Open Access Article. Published on 07 2020. Downloaded on 2025/12/13 4:57:53.
This article is licensed under a Creative Commons Attribution-NonCommercial 3.0 Unported Licence.

A. E. Gorbalenya, E. J. Snijder and R. A. Fouchier, *mBio*, 2012, **3**(6), e00473-12.

40 A. E. Gorbalenya, L. Enjuanes, J. Ziebuhr and E. J. Snijder, *Virus Res.*, 2006, **117**, 17–37.

41 E. J. Snijder, P. J. Bredenbeek, J. C. Dobbe, V. Thiel, J. Ziebuhr, L. L. M. Poon, Y. Guan, M. Rozanov, W. J. M. Spaan and A. E. Gorbalenya, *J. Mol. Biol.*, 2003, **331**, 991–1004.

42 J. Ziebuhr, E. J. Snijder and A. E. Gorbalenya, *J. Gen. Virol.*, 2000, **81**, 853–879.

43 Z. Song, Y. Xu, L. Bao, L. Zhang, P. Yu, Y. Qu, H. Zhu, W. Zhao, Y. Han and C. Qin, *Viruses*, 2019, **11**, 59.

44 S. Jiang, L. Lu, L. Du and A. K. Debnath, *J. Infect.*, 2013, **66**, 464–466.

45 V. S. Raj, H. Mou, S. L. Smits, D. H. Dekkers, M. A. Muller, R. Dijkman, D. Muth, J. A. Demmers, A. Zaki, R. A. Fouchier, V. Thiel, C. Drosten, P. J. Rottier, A. D. Osterhaus, B. J. Bosch and B. L. Haagmans, *Nature*, 2013, **495**, 251–254.

46 N. Wang, X. Shi, L. Jiang, S. Zhang, D. Wang, P. Tong, D. Guo, L. Fu, Y. Cui, X. Liu, K. C. Arledge, Y. H. Chen, L. Zhang and X. Wang, *Cell Res.*, 2013, **23**, 986–993.

47 S. H. Havale and M. Pal, *Bioorg. Med. Chem.*, 2009, **17**, 1783–1802.

48 J. Ling, L. Ge, D. H. Zhang, Y. F. Wang, Z. L. Xie, J. H. Tian, X. H. Xiao and K. H. Yang, *Acta Diabetol.*, 2019, **56**, 7–27.

49 C. F. Deacon, *Nat. Rev. Endocrinol.*, 2020, **16**, 642–653.

50 D. Forni, G. Filippi, R. Cagliani, L. De Gioia, U. Pozzoli, N. Al-Daghri, M. Clerici and M. Sironi, *Sci. Rep.*, 2015, **5**, 14480.

51 G. Zhao, L. Du, C. Ma, Y. Li, L. Li, V. K. Poon, L. Wang, F. Yu, B. J. Zheng, S. Jiang and Y. Zhou, *J. Virol.*, 2013, **10**, 266.

52 J. M. Garcia, A. Gao, P. L. He, J. Choi, W. Tang, R. Bruzzone, O. Schwartz, H. Naya, F. J. Nan, J. Li, R. Altmeyer and J. P. Zuo, *Antiviral Res.*, 2009, **81**, 239–247.

53 G. Bort, M. Sylla-Iyarreta Veitía and C. Ferroud, *Tetrahedron*, 2013, **69**, 7345–7353.

54 M. Singh, S. K. Singh, B. Thakur, P. Ray and S. K. Singh, *Anti-Cancer Agents Med. Chem.*, 2016, **16**, 722–739.

55 K. Potgieter, T. Gerber, E. Hosten and R. Betz, *Acta Crystallogr., Sect. E: Struct. Rep. Online*, 2012, **68**, o27.